

# Revisiting Locally Differentially Private Protocols: Towards Better Trade-offs in Privacy, Utility, and Attack Resistance

Héber H. Arcolezzi

Inria Centre at the University Grenoble Alpes  
France  
heber.hwang-arcolezzi@inria.fr

Sébastien Gambs

Université du Québec à Montréal (UQAM)  
Canada  
gambs.sebastien@uqam.ca

**Abstract**—Local Differential Privacy (LDP) offers strong privacy protection, especially in settings in which the server collecting the data is untrusted. However, designing LDP mechanisms that achieve an optimal trade-off between privacy, utility and robustness to adversarial inference attacks remains challenging. In this work, we introduce a general multi-objective optimization framework for refining LDP protocols, enabling the joint optimization of privacy and utility under various adversarial settings. While our framework is flexible to accommodate multiple privacy and security attacks as well as utility metrics, in this paper, we specifically optimize for Attacker Success Rate (ASR) under data reconstruction attack as a concrete measure of privacy leakage and Mean Squared Error (MSE) as a measure of utility. More precisely, we systematically revisit these trade-offs by analyzing eight state-of-the-art LDP protocols and proposing refined counterparts that leverage tailored optimization techniques. Experimental results demonstrate that our proposed adaptive mechanisms consistently outperform their non-adaptive counterparts, achieving substantial reductions in ASR while preserving utility, and pushing closer to the ASR-MSE Pareto frontier. By bridging the gap between theoretical guarantees and real-world vulnerabilities, our framework enables modular and context-aware deployment of LDP mechanisms with tunable privacy-utility trade-offs.

## I. INTRODUCTION

Differential Privacy (DP) [1] has become a gold standard for preserving privacy in data analytics and mining, in which the goal is to ensure that an individual’s data does not significantly influence the output of any analysis. However, traditional DP relies on a trusted aggregator to apply the privacy mechanism, which is often impractical for decentralized or privacy-sensitive applications. This limitation has led to the rise of Local Differential Privacy (LDP) [2], a model that removes the need for a trusted aggregator by requiring users to perturb their data locally before sharing it with the server.

The local DP model has gained widespread adoption, with major technology companies integrating it into their systems to enhance user privacy. Notable examples include Google Chrome [3] and Windows 10 [4], in which LDP protocols have been used to collect statistics while safeguarding individual data. A fundamental task under LDP guarantees is **frequency estimation**, which forms the basis of many advanced data analysis tasks like heavy hitter estimation [5]–[7], frequency

monitoring [3], [4], [8], [9], multidimensional queries [10]–[13], frequent item-set mining [14], [15] and spatial density estimation [16], [17].

Due to its importance, numerous LDP frequency estimation protocols have been proposed [18], namely, Generalized Randomized Response (GRR) [19], Subset Selection (SS) [20], [21], Symmetric Unary Encoding (SUE) [3], Optimized Unary Encoding (OUE) [22], Summation with Histogram Encoding (SHE) [1], Thresholding with Histogram Encoding (THE) [22], Binary Local Hashing (BLH) [5] and Optimal Local Hashing (OLH) [22]. These protocols mainly focus on improving utility, often quantified in terms of the variance (*i.e.*, Mean Squared Error – MSE), as well as optimizing computational and communication costs [23], [24] to enable efficient data collection in large-scale systems.

While utility and communication costs have been the traditional focus of LDP frequency estimation protocols, recent research has shed light on their vulnerabilities in adversarial settings. For instance, **re-identification risks** [25], [26] have shown that adversaries can uniquely identify users within a dataset, while **attribute inference attacks** [9], [27], [28] have been explored in the context of iterative data collections. Furthermore, recent works have examined **data reconstruction attacks** [26], [28], [29], in which adversaries aim to recover the user’s original input from its obfuscated output. Among these threats, we focus specifically on data reconstruction attacks, which are particularly critical, as they represent a **worst-case leakage scenario**: if an attacker can recover the user’s data from a single report, other adversaries with access to side information or repeated queries can only perform better.

**Contributions.** In this work, *we introduce a general multi-objective optimization framework for refining LDP frequency estimation protocols*, enabling the joint optimization of privacy and utility under various adversarial settings. While our framework is flexible enough to incorporate multiple objectives, in this paper we focus on data reconstruction attacks [26], [28], [29] quantified by the Attacker Success Rate (ASR), and utility measured via Mean Squared Error (MSE). As aforementioned, data reconstruction attacks are particularly relevant as they directly challenge the fundamental

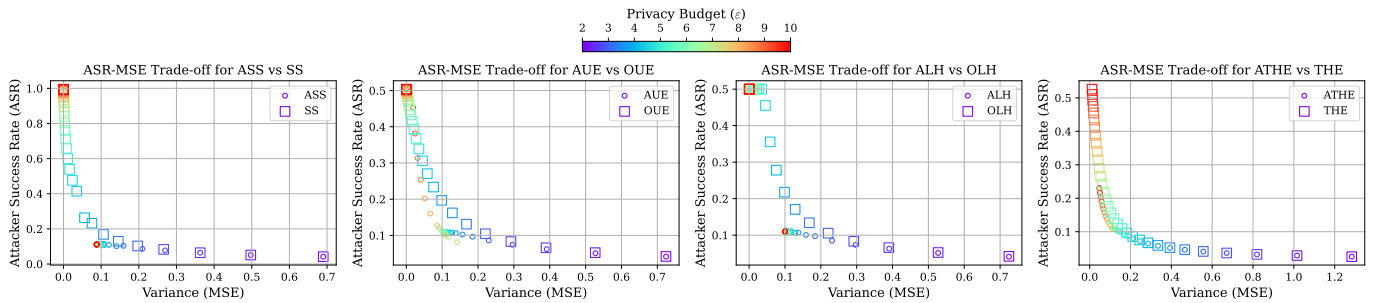


Fig. 1: Comparison of data reconstruction attack (*i.e.*, ASR) vs. variance (*i.e.*, MSE) for four state-of-the-art LDP protocols (SS [20], [21], OUE [22], OLH [22], THE [22]) and our newly proposed adaptive versions (ASS, AUE, ALH, ATHE). Each subplot considers a range of privacy budgets  $\epsilon \in (2, 10)$  and a fixed domain size  $k = 100$ . Our adaptive protocols (indicated by  $\circ$  markers) yield substantially lower ASR at the same or close levels of MSE when compared to their original counterparts (indicated by  $\square$  markers). This improvement is reflected in the adaptive protocols’ proximity to the Pareto frontier, indicating a more favorable privacy-utility trade-off and reduced vulnerability to privacy attacks.

goal of LDP: preventing an adversary from inferring a user’s value from the obfuscated output. Meanwhile, MSE serves as a widely adopted utility metric in LDP literature [22], [30], [31] due to its analytical tractability and connection to other estimation measures, such as Mean Absolute Error (MAE) and Fisher Information [19], [32] (the rationale for choosing these metrics is further discussed in Section V-B).

To demonstrate the practical benefits of our framework, **we refine four state-of-the-art LDP protocols** (SS, OUE, OLH and THE), by proposing adaptive versions, namely, ASS, AUE, ALH and ATHE, which achieve superior trade-off between privacy and utility compared to their traditional counterparts (*e.g.*, see Figure 1). Additionally, we derive the expected data reconstruction attack (*i.e.*, analytical ASR) for three additional LDP protocols (SHE, THE and a generic Unary Encoding protocol), extending prior analyses [28], [29]. Our refined protocols offer enhanced robustness against privacy attacks while maintaining practical utility levels, demonstrating the effectiveness of our framework in optimizing LDP mechanisms beyond conventional single-objective approaches. The main contributions of this paper can be summarized as follows:

- We introduce a **general multi-objective optimization framework** that enables the joint optimization of privacy and utility in LDP frequency estimation. Our framework is designed to assist practitioners in deploying LDP mechanisms with customized privacy-utility trade-offs, acting as a tuning layer adaptable to various systems (*e.g.*, telemetry collection, mobile analytics).
- We **extend four state-of-the-art LDP frequency estimation protocols**—SS, OUE, OLH and THE—by proposing refined versions named ASS, AUE, ALH and ATHE. These refined protocols offer a significantly better trade-off between robustness to privacy attacks and utility compared to their traditional counterparts (*e.g.*, see Figure 1).
- We derive the **analytical closed-form equation** of the expected data reconstruction attack for three LDP protocols going beyond previous works [28]. These derivations are critical for evaluating and optimizing the guarantees

of LDP protocols under adversarial inference scenarios.

- We validate our proposed adaptive protocols **through extensive experiments**, demonstrating their effectiveness in achieving a more favorable balance between privacy (ASR) and utility (MSE) compared to existing protocols, under the same  $\epsilon$ -LDP guarantees. Our results indicate that the refined protocols can substantially reduce adversarial success rates while maintaining competitive estimation accuracy.

**Outline.** The remainder of this paper is structured as follows. First, Section II reviews the most relevant related work, providing context for our contributions. Next, Section III defines the problem, introduces the LDP privacy model and describes the adversarial model used in this study. Section IV provides an overview of the eight LDP frequency estimation protocols analyzed in this work, along with their attack models. Section V then presents our multi-objective framework and the proposed adaptive LDP protocols that refine the original methods to enhance privacy and utility. Afterward, Section VI details the experiments conducted and presents a comprehensive analysis of the results. Finally, Section VII concludes the paper and discusses future research.

## II. RELATED WORK

Frequency estimation is one of the primary objective of LDP, serving as a building block for a wide range of advanced applications, such as heavy hitter estimation [5]–[7], frequency monitoring [3], [4], [8], [9], multidimensional queries [10]–[13], frequent item-set mining [14], [15], and spatial density estimation [16], [17]. Numerous LDP frequency estimation protocols have been proposed in the literature [19]–[24], [31], primarily focusing on minimizing estimation error, computational cost, or communication overhead. However, recent studies started to examine LDP frequency estimation mechanisms from an adversarial perspective such as data reconstruction attacks [26], [28], [29], re-identification risks [25], [26], attribute inference attacks [9], [27], [33] and poisoning attacks [34]. Our focus is on data reconstruction attacks, which allow

adversaries to predict the user’s input based on the observed obfuscated output. However, unlike these prior studies that primarily highlight vulnerabilities, we propose a systematic methodology to refine existing protocols, thus reducing their susceptibility to known and emerging privacy threats.

Specifically, our work differs from the existing data reconstruction attack literature [26], [28], [29] in the following aspects. First, we formally analyze three LDP protocols’ expected ASR beyond the ones in [28]. Second, we extensively analyzed the privacy, utility, and robustness against privacy attacks of eight state-of-the-art LDP protocols. Third, we formulate a multi-objective optimization problem for LDP frequency estimation protocols instead of the single-objective one (*i.e.*, utility-driven). This allowed us to propose four new adaptive and refined LDP protocols, which provide better trade-offs in terms of privacy, utility, and robustness against adversarial attacks.

### III. BACKGROUND

**Notation.** We use italic uppercase letters (*e.g.*,  $U$ ) to denote sets, and write  $[n] = \{1, \dots, n\}$  to represent a set of  $n$  positive integers. Vectors are denoted by bold lowercase letters (*e.g.*,  $\mathbf{x}$ ), where  $x_i$  represents the value of the  $i$ -th coordinate of  $\mathbf{x}$ . Finally, randomized mechanisms are denoted by  $\mathcal{M}$ , the input domain is denoted by  $\mathcal{X}$ , and the output domain by  $\mathcal{Y}$ . Both  $\mathcal{X}$  and  $\mathcal{Y}$  are discrete, in which  $|\mathcal{X}| = k$  and  $|\mathcal{Y}|$  depends on the randomized mechanism  $\mathcal{M}$ .

#### A. Problem Statement

We consider an untrusted server collecting data from a distributed group of users while preserving their privacy. Formally, there are  $n$  users, with each user holding a value  $x$  from a discrete domain  $\mathcal{X} = \{1, 2, \dots, k\}$ . The task is **frequency estimation**, in which the server aims to learn the frequencies of each value across all users, denoted as  $\mathbf{f} = \{f_i\}_{i \in [k]}$ .

- **Users’ goal.** Each user wants to protect their privacy. To achieve this, users apply an obfuscation mechanism  $\mathcal{M}$  that perturbs their value  $x$  before sending it to the server.
- **Server’s objective.** The server aims to estimate the frequency distribution  $\mathbf{f}$  of the values held by all users while minimizing the estimation error. After receiving the obfuscated values from all  $n$  users, the server estimates a  $k$ -bins histogram  $\hat{\mathbf{f}} = \{\hat{f}_i\}_{i \in [k]}$ , representing the estimated frequencies.
- **Adversary’s goal.** The adversary aims to accurately infer each user’s true value  $x \in \mathcal{X}$  based on the obfuscated output  $y \in \mathcal{Y}$  sent to the server (*i.e.*, data reconstruction attack).

This threat model captures a worst-case adversary (*e.g.*, a corrupted or server itself a man-in-the-middle adversary) who observes the user’s obfuscated report and aims to infer the original input without auxiliary information, reflecting a realistic scenario in distributed or untrusted settings.

#### B. Local Differential Privacy

Local Differential Privacy (LDP) [2] ensures that the output of a randomized mechanism does not significantly reveal information about the input. Formally:

**Definition 1** ( $\epsilon$ -Local Differential Privacy). *An algorithm  $\mathcal{M}$  satisfies  $\epsilon$ -local differential privacy ( $\epsilon$ -LDP), where  $\epsilon \geq 0$ , if and only if for any two distinct inputs  $x, x' \in \mathcal{X}$ , we have:*

$$\forall y \in \text{Range}(\mathcal{M}) : \Pr[\mathcal{M}(x) = y] \leq e^\epsilon \cdot \Pr[\mathcal{M}(x') = y], \quad (1)$$

in which  $\text{Range}(\mathcal{M})$  denotes the set of all possible outputs of  $\mathcal{M}$ .

Smaller values of  $\epsilon$  indicate stronger privacy guarantees, as they limit how much more likely the output is for one input compared to another given the same observed value. In other words,  $\epsilon$  controls the level of indistinguishability between inputs  $x$  and  $x'$ , providing a formal measure of privacy.

#### C. Pure LDP Framework

We consider the pure LDP framework proposed by Wang and co-authors [22] to analyze LDP frequency estimation protocols. Formally, an LDP protocol is called pure if it satisfies the following definition:

**Definition 2** (Pure LDP Protocols [22]). *A protocol is considered pure if and only if there exist two probability values,  $p^* > q^*$ , in its perturbation mechanism  $\mathcal{M}$ , such that for all inputs  $x \in \mathcal{X}$ :*

$$\begin{aligned} \Pr[\mathcal{M}(x) \in \{y \mid x \in \text{Support}(y)\}] &= p^* \\ \forall x' \neq x \Pr[\mathcal{M}(x') \in \{y \mid x \in \text{Support}(y)\}] &= q^* \end{aligned}$$

in which the set  $\{y \mid x \in \text{Support}(y)\}$  includes all possible outputs  $y$  that “support” the input value  $x$ .

Thus,  $p^*$  represents the probability that the input  $x$  is mapped to an output supporting it, whereas  $q^*$  represents the probability that any other input  $x' \neq x$  is mapped to an output that supports  $x$ . Given  $n$  users, let  $y^j$  denote the obfuscated value of user  $j \in [n]$ , the frequency estimate  $\hat{f}_i$  of the input value  $i \in [k]$  is computed as:

$$\hat{f}_i = \frac{\sum_{j=1}^n \mathbb{1}_{\text{Support}(y^j)}(i) - nq^*}{n(p^* - q^*)}. \quad (2)$$

As shown in [22], the estimator in Equation (2) is unbiased (*i.e.*,  $\mathbb{E}[\hat{f}_i] = f_i$ ) and the variance of the estimation  $\hat{f}_i$  is:

$$\text{Var}[\hat{f}_i] = \frac{q^*(1 - q^*)}{n(p^* - q^*)^2} + \frac{f_i(1 - p^* - q^*)}{n(p^* - q^*)}. \quad (3)$$

With a sufficiently large domain size and no dominant frequency  $f_i$ , the second term of Equation (3) can be ignored. Thus, as commonly used in the LDP literature [8], [11], [22], we will consider the approximate variance, which is given by:

$$\text{Var}[\hat{f}_i] \approx \frac{q^*(1 - q^*)}{n(p^* - q^*)^2}. \quad (4)$$

Furthermore, as the estimation is unbiased, we will interchangeably refer to the variance as the MSE:

$$\text{MSE} = \frac{1}{k} \sum_{i=1}^k \mathbb{E} \left[ \left( \hat{\mathbf{f}}_i - \mathbf{f}_i \right)^2 \right] = \frac{1}{k} \sum_{i=1}^k \text{Var}[\hat{\mathbf{f}}_i].$$

#### D. Data Reconstruction Attack on LDP

The fundamental premise of  $\varepsilon$ -LDP, as stated in Equation (1), is that the input to  $\mathcal{M}$  cannot be confidently determined from its output, with the level of confidence determined by  $e^\varepsilon$ . Therefore, the user's privacy is considered compromised if an adversary  $\mathcal{A}$  can successfully infer the user's original input  $x \in \mathcal{X}$  from the obfuscated output  $y \in \mathcal{Y}$ . While various adversarial models have been proposed to exploit vulnerabilities in LDP mechanisms, including re-identification [25], [26] and poisoning [34] attacks, in this paper, and without loss of generality, we focus on data reconstruction attacks [26], [28], [29]. These attacks provide a fundamental measure of privacy leakage in LDP, as they directly **quantify how well an adversary can infer the true input from the obfuscated response**. Formally, the adversary's prediction  $\hat{x}$  can be defined as:

$$\hat{x} = \arg \max_{x \in \mathcal{X}} \Pr[x | y].$$

By applying Bayes' theorem, we rewrite the expression as:

$$\hat{x} = \arg \max_{x \in \mathcal{X}} \frac{\Pr[y | x] \cdot \Pr[x]}{\Pr[y]}.$$

Assuming a uniform prior distribution over  $x$  (i.e.,  $\Pr[x] = \frac{1}{k}$ , where  $k = |\mathcal{X}|$ ), and noting that  $\Pr[y]$  is constant for a given observation, the expression simplifies to:

$$\hat{x} = \arg \max_{x \in \mathcal{X}} \Pr[y | x].$$

To assess the accuracy of the attack, we will use the **Attacker Success Rate (ASR)** metric, which represents the probability that the adversary's prediction  $\hat{x}$  matches the input value  $x$  (i.e., correctly reconstructs the users' data):

$$\text{ASR} = \Pr[\hat{x} = x] = \frac{1}{n} \cdot \sum_{j=1}^n \mathbb{1}(\hat{x}^j = x^j).$$

Mathematically, it is also possible to derive the **expected data reconstruction attack** for each protocol through formal expected value analysis [28]:

$$\mathbb{E}[\text{ASR}] = \mathbb{E}[\Pr[\hat{x} = x]].$$

With ASR, we can assess LDP protocols' effectiveness in protecting privacy, uncovering vulnerabilities not evident from  $\varepsilon$  alone.

## IV. LDP FREQUENCY ESTIMATION PROTOCOLS

In this section, we provide a concise overview of eight state-of-the-art LDP frequency estimation protocols. We systematically describe each mechanism based on three key functions: **Encoding**, **Perturbation** and **Aggregation** which collectively define their operation. Additionally, we introduce an **Attacking** function for each protocol, highlighting potential

vulnerabilities to privacy attacks. For protocols in which the expected ASR is not available in the literature [28], we derive it and present the detailed analyses in Appendix A.

#### A. Generalized Randomized Response (GRR)

GRR [19] extends the randomized response method proposed by Warner [35] to a domain size of  $k \geq 2$ , while ensuring  $\varepsilon$ -LDP.

**Encoding.** In GRR,  $\text{Encode}(x) = x$  and  $x \in [k]$ .

**Perturbation.** The perturbation function of GRR is given by:

$$\Pr[\text{GRR}(x) = y] = \begin{cases} p = \frac{e^\varepsilon}{e^\varepsilon + k - 1} & \text{if } y = x, \\ q = \frac{1}{e^\varepsilon + k - 1} & \text{if } y \neq x, \end{cases} \quad (5)$$

in which  $y \in [k]$  is the perturbed value sent to the server.

**Aggregation.** In GRR, each output value  $i$  supports the corresponding input  $i$ , resulting in the support set  $\mathbb{1}_{\text{GRR}} = y$ . GRR is a pure protocol with  $p^* = p$  and  $q^* = q$ . The server estimates the frequency using Equation (2), with the following analytical MSE:

$$\text{MSE}_{\text{GRR}} = \frac{e^\varepsilon + k - 2}{n(e^\varepsilon - 1)^2}. \quad (6)$$

**Attacking.** From Equation (5), it follows that  $\Pr[y = x] > \Pr[y = x']$  for all  $x' \in \mathcal{X} \setminus \{x\}$ . Thus, the optimal attack strategy for GRR is to predict  $\hat{x} = \mathcal{A}_{\text{GRR}}(y) = y$ . The expected ASR for GRR is given by:

$$\mathbb{E}[\text{ASR}]_{\text{GRR}} = \frac{e^\varepsilon}{e^\varepsilon + k - 1}. \quad (7)$$

#### B. Subset Selection (SS)

SS [20], [21] outputs a randomly selected subset  $\mathbf{y}$  of size  $\omega$  from the original domain  $\mathcal{X}$ . SS can be seen as a generalization and optimization of GRR, in which SS is equivalent to GRR when  $\omega = 1$ .

**Encoding and Perturbation.** Starting with an empty subset  $\mathbf{y} = \emptyset$ , the true value  $x$  is added to  $\mathbf{y}$  with probability:  $p = \frac{\omega e^\varepsilon}{\omega e^\varepsilon + k - \omega}$ . Finally, values are added to  $\mathbf{y}$  as follows:

- If  $x \in \mathbf{y}$ , then  $\omega - 1$  values are sampled from  $\mathcal{X} \setminus \{x\}$  uniformly at random (without replacement) and are added to  $\mathbf{y}$ ;
- If  $x \notin \mathbf{y}$ , then  $\omega$  values are sampled from  $\mathcal{X} \setminus \{x\}$  uniformly at random (without replacement) and are added to  $\mathbf{y}$ .

The user then sends the subset  $\mathbf{y}$  to the server.

**Aggregation.** In SS, each value  $i$  in the output subset  $\mathbf{y}$  supports the corresponding input value  $i$ . Thus, the support set for SS is  $\mathbb{1}_{\text{SS}} = \{x | x \in \mathbf{y}\}$ . This protocol is pure, with:  $p^* = p = \frac{\omega e^\varepsilon}{\omega e^\varepsilon + k - \omega}$  and  $q^* = \frac{\omega e^\varepsilon (\omega - 1) + (k - \omega) \omega}{(k - 1)(\omega e^\varepsilon + k - \omega)}$ . The server estimates the frequency using Equation (2), with the following analytical MSE:

$$\text{MSE}_{\text{SS}} = \left( \frac{(k - 1)(k + 2\omega e^\varepsilon - \omega)}{n\omega(-k + \omega + (k - 1)e^\varepsilon - (\omega - 1)e^\varepsilon)^2} + \frac{(k - \omega + (\omega - 1)e^\varepsilon)(-\omega(k - \omega) - \omega(\omega - 1)e^\varepsilon)}{n\omega(-k + \omega + (k - 1)e^\varepsilon - (\omega - 1)e^\varepsilon)^2} \right). \quad (8)$$

The optimal subset size that minimizes the MSE of SS in Equation (8) is  $\omega = \max\left(1, \left\lfloor \frac{k}{e^\varepsilon + 1} \right\rfloor\right)$  [20], [21].

**Attacking.** With the support set of each user's report  $\mathbb{1}_{\text{SS}}$ , the optimal attack strategy  $\mathcal{A}_{\text{SS}}$  is to predict  $\hat{x} = \text{Uniform}(\mathbb{1}_{\text{SS}})$  [26], [28]. The expected ASR for SS is [28]:

$$\mathbb{E}[\text{ASR}]_{\text{SS}} = \frac{e^\varepsilon}{\omega e^\varepsilon + k - \omega}. \quad (9)$$

#### C. Unary Encoding (UE)

UE protocols [3], [22] encode the user's input  $x \in \mathcal{X}$  as a  $k$ -dimensional one-hot vector  $\mathbf{x}$ , in which each bit is subsequently obfuscated independently.

**Encoding.**  $\text{Encode}(x) = [0, \dots, 0, 1, 0, \dots, 0]$  is a binary vector with a single 1 at position  $x$  and all other positions set to 0.

**Perturbation.** The obfuscation function of UE mechanisms randomizes the bits from  $\mathbf{x}$  independently to generate  $\mathbf{y}$  as:

$$\forall i \in [k]: \quad \Pr[\mathbf{y}_i = 1] = \begin{cases} p, & \text{if } \mathbf{x}_i = 1, \\ q, & \text{if } \mathbf{x}_i = 0, \end{cases} \quad (10)$$

in which  $\mathbf{y}$  is sent to the server. There are two variations of UE mechanisms: (i) Symmetric UE (SUE) [3] that selects  $p = \frac{e^{\varepsilon/2}}{e^{\varepsilon/2} + 1}$  and  $q = \frac{1}{e^{\varepsilon/2} + 1}$ ; and (ii) Optimized UE (OUE) [22] that selects  $p = \frac{1}{2}$  and  $q = \frac{1}{e^\varepsilon + 1}$  to minimize the MSE in Equation (11) below.

**Aggregation.** A reported bit vector  $\mathbf{y}$  is considered to support an input  $i$  if  $\mathbf{y}_i = 1$ . Therefore, the support set for UE protocols is defined as  $\mathbb{1}_{\text{UE}} = \{i | \mathbf{y}_i = 1\}$ . UE protocols are pure with  $p^* = p$  and  $q^* = q$ . The server estimates the frequency using Equation (2), with the corresponding MSE as:

$$\text{MSE}_{\text{UE}} = \frac{((e^\varepsilon - 1)q + 1)^2}{n(e^\varepsilon - 1)^2(1 - q)q}. \quad (11)$$

**Attacking.** Given the support set of each user's report,  $\mathbb{1}_{\text{UE}}$ , the adversary can adopt two possible attack strategies  $\mathcal{A}_{\text{UE}}$  [26], [28]:

- $\mathcal{A}_{\text{UE}}^0$  is a random choice  $\hat{x} = \text{Uniform}([k])$ , if  $\mathbb{1}_{\text{UE}} = \emptyset$ ;
- $\mathcal{A}_{\text{UE}}^1$  is a random choice  $\hat{x} = \text{Uniform}(\mathbb{1}_{\text{UE}})$ , otherwise.

In this paper, we generalized the expected ASR of SUE and OUE given in [28] for any UE protocol as:

$$\mathbb{E}[\text{ASR}]_{\text{UE}} = (1 - p) \cdot (1 - q)^{k-1} \cdot \frac{1}{k} + \sum_{m=1}^k p \cdot \frac{1}{m} \cdot \binom{k-1}{m-1} q^{m-1} (1 - q)^{(k-1)-(m-1)}. \quad (12)$$

We defer the derivation of Equation 12 to Appendix A1.

#### D. Local Hashing (LH)

LH protocols [5], [22] use hash functions to map the input data  $x \in \mathcal{X}$  to a new domain  $[g]$ , and then obfuscates the hash value with GRR. Let  $\mathcal{H}$  be a universal hash function family such that each hash function  $H \in \mathcal{H}$  hashes a value  $x \in \mathcal{X}$  into  $[g]$  (i.e.,  $H: [k] \rightarrow [g]$ ).

**Encoding.**  $\text{Encode}(x) = \langle H, h \rangle$ , in which  $H \in \mathcal{H}$  is chosen uniformly at random, and  $h = H(x)$ . There are two variations of LH mechanisms: (i) Binary LH (BLH) [5] that just sets  $g = 2$ , and (ii) Optimized LH (OLH) [22] that selects  $g = \lfloor e^\varepsilon + 1 \rfloor$  to minimize the MSE in Equation (14) below.

**Perturbation.** LH protocols perturb  $\langle H, h \rangle$  into  $\langle H, y \rangle$ , just like GRR, as follows:

$$\forall i \in [g], \quad \Pr[y = i] = \begin{cases} p = \frac{e^\varepsilon}{e^\varepsilon + g - 1}, & \text{if } h = i, \\ q = \frac{1}{e^\varepsilon + g - 1}, & \text{if } h \neq i. \end{cases} \quad (13)$$

**Aggregation.** For each reported tuple  $\langle H, y \rangle$ , the support set for LH protocols consists of all values  $x \in \mathcal{X}$  that hash to  $y$ , denoted as  $\mathbb{1}_{\text{LH}} = \{x | H(x) = y\}$ . LH protocols are pure with  $p^* = p$  and  $q^* = \frac{1}{g}$ . The server estimates the frequency using Equation (2) with the following analytical MSE:

$$\text{MSE}_{\text{LH}} = \frac{(e^\varepsilon - 1 + g)^2}{n(e^\varepsilon - 1)^2(g - 1)}. \quad (14)$$

**Attacking.** Based on the support set of each user's report,  $\mathbb{1}_{\text{LH}}$ , the adversary can employ one of two possible attack strategies, denoted by  $\mathcal{A}_{\text{LH}}$  [26], [28]:

- $\mathcal{A}_{\text{LH}}^0$  is a random choice  $\hat{x} = \text{Uniform}([k])$ , if  $\mathbb{1}_{\text{LH}} = \emptyset$ ;
- $\mathcal{A}_{\text{LH}}^1$  is a random choice  $\hat{x} = \text{Uniform}(\mathbb{1}_{\text{LH}})$ , otherwise.

The expected ASR of LH protocols is given by [28]:

$$\mathbb{E}[\text{ASR}]_{\text{LH}} = \frac{e^\varepsilon}{(e^\varepsilon + g - 1) \cdot \max\left\{\frac{k}{g}, 1\right\}}. \quad (15)$$

#### E. Histogram Encoding (HE)

HE protocols [22] encode the user's input data  $x \in \mathcal{X}$ , as a one-hot  $k$ -dimensional histogram before obfuscating each bit independently.

**Encoding.**  $\text{Encode}(x) = [0.0, 0.0, \dots, 1.0, 0.0, \dots, 0.0]$  in which only the  $x$ -th component is 1.0. Two different input values  $x, x' \in \mathcal{X}$  will result in two vectors with L1 distance of  $\Delta_1 = 2$ .

**Perturbation.** The perturbation function  $\text{Perturb}(\mathbf{x})$  generates the output vector  $\mathbf{y}$ , where each component is given by  $\mathbf{y}_i = \mathbf{x}_i + \text{Lap}\left(\frac{\Delta_1}{\varepsilon}\right)$ , with  $\text{Lap}(\cdot)$  representing the Laplace mechanism [1].

The following subsections describe two HE-based mechanisms: Summation with HE (SHE) and Thresholding with HE (THE). These mechanisms differ in their aggregation and attack strategies.

1) *Summation with HE (SHE):* With SHE, there is no post-processing of  $\mathbf{y}$  at the server side.

**Aggregation.** Since Laplace noise with mean 0 is added to each vector independently, the server estimates the frequency using the sum of the noisy reports:  $\hat{\mathbf{f}} = \left\{ \sum_{j=1}^n \mathbf{y}_i^j \right\}_{i \in [k]}$ . This aggregation method for SHE does not provide a support set and is not pure. The analytical MSE of this estimation is:

$$\text{MSE}_{\text{SHE}} = \frac{8}{n\varepsilon^2}. \quad (16)$$

**Attacking.** The optimal attack strategy for SHE is to predict the user's value by selecting the index corresponding to the maximum component of the obfuscated vector:

$\hat{x} = \underset{i \in [k]}{\operatorname{argmax}} y_i$  [29]. Following this attack strategy, we deduce the expected ASR for the SHE protocol as the probability that the noisy value  $y_x$  at the true index exceeds all other noisy values  $y_i$  for  $i \neq x$ :

$$\mathbb{E}[\text{ASR}]_{\text{SHE}} = \Pr \left[ y_x > \max_{i \neq x} y_i \right]. \quad (17)$$

We defer the derivation of Equation (17) to Appendix A2.

2) *Thresholding with HE (THE)*: In THE, each perturbed component of the vector  $\mathbf{y}$  is compared to a threshold value  $\theta$  to generate the final output vector. More precisely:

$$\forall i \in [k]: \quad \mathbf{y}_i = \begin{cases} 1, & \text{if } \mathbf{y}_i > \theta \\ 0, & \text{if } \mathbf{y}_i \leq \theta \end{cases}$$

Thus, the resulting output vector  $\mathbf{y}$  is a binary vector in  $\{0, 1\}^k$ , where we have the following probabilities:

$$p = \Pr[\mathbf{y}_i = 1 \mid \mathbf{x}_i = 1] = 1 - \frac{1}{2} e^{\frac{\varepsilon}{2}(\theta-1)}. \quad (18)$$

$$q = \Pr[\mathbf{y}_i = 1 \mid \mathbf{x}_i = 0] = \frac{1}{2} e^{-\frac{\varepsilon}{2}\theta}. \quad (19)$$

**Aggregation.** A reported bit vector  $\mathbf{y}$  is viewed as supporting an input  $i$  if  $\mathbf{y}_i > \theta$ . Therefore, the support set for THE is  $\mathbb{1}_{\text{THE}} = \{i \mid \mathbf{y}_i > \theta\}$ . The THE mechanism is pure with  $p^* = p$  and  $q^* = q$ . The server estimates the frequency using Equation (2) with the following analytical MSE:

$$\text{MSE}_{\text{THE}} = \frac{2e^{\varepsilon\theta/2} - 1}{n(1 + e^{\varepsilon(\theta-1/2)} - 2e^{\varepsilon\theta/2})^2}. \quad (20)$$

The optimal threshold value that minimizes the protocol's MSE in Equation (20) is within  $\theta \in (0.5, 1)$  [22].

**Attacking.** Based on the support set  $\mathbb{1}_{\text{THE}}$ , the adversary can use one of two attack strategies denoted by  $\mathcal{A}_{\text{THE}}$  [29]:

- $\mathcal{A}_{\text{THE}}^0$  is a random choice  $\hat{x} = \text{Uniform}([k])$ , if  $\mathbb{1}_{\text{THE}} = \emptyset$ ;
- $\mathcal{A}_{\text{THE}}^1$  is a random choice  $\hat{x} = \text{Uniform}(\mathbb{1}_{\text{THE}})$ , otherwise.

In this paper, we obtained the expected ASR for THE as:

$$\mathbb{E}[\text{ASR}]_{\text{THE}} = (1-p)(1-q)^{k-1} \cdot \frac{1}{k} + \frac{p}{kq} (1 - (1-q)^k). \quad (21)$$

We defer the derivation of Equation (21) to Appendix A3.

## V. REFINING LDP PROTOCOLS

The existing literature has traditionally proposed mechanisms like SS, OUE, OLH and THE, focusing solely on minimizing MSE for a given privacy budget  $\varepsilon$ . However, these protocols exhibit varying vulnerabilities to privacy and security attacks under the same  $\varepsilon$  value, leaving room for improvement in both privacy guarantees and estimation accuracy. To address this, we introduce a **general multi-objective optimization framework** for refining LDP frequency estimation protocols, enabling adaptive parameter tuning based on multiple privacy and utility considerations.

### A. Multi-Objective Optimization Framework

We frame the protocol refinement as a general multi-objective optimization problem, in which the goal is to jointly minimize a set of metrics that characterize distinct desirable properties:

$$\min_{\theta \in \Theta} (\mathcal{P}(\theta), \mathcal{U}(\theta), \mathcal{S}(\theta), \mathcal{C}(\theta)), \text{ in which} \quad (22)$$

- $\mathcal{P}$  quantifies the LDP protocol's vulnerability to **privacy attacks**, such as reconstruction [28], [29], inference [9], [27], [33] or re-identification [25], [26];
- $\mathcal{U}$  reflects **utility degradation**, often via MSE, Mean Absolute Error (MAE) [19], or Fisher Information [32];
- $\mathcal{S}$  captures **security robustness** to adversarial manipulation [36] or data poisoning [34];
- $\mathcal{C}$  measures **communication cost**, *e.g.*, bandwidth or message size [23].

Each dimension may be relevant depending on the application context, and the goal is to explore **Pareto-efficient solutions** that avoids sacrificing one objective disproportionately for gains in another.

### B. Specialization to Data Reconstruction and MSE Trade-off

While the full multi-objective framework in Section V-A is general, in this paper we focus on a widely applicable and analytically tractable two-objective setting. Specifically, we optimize the trade-off between:

- **Privacy attacks**, measured via the ASR under *data reconstruction*, which is the most fundamental and consequential threat in privacy-preserving data analysis [37]–[39]. Their severity lies in the fact that once an adversary successfully reconstructs individual-level data, a wide range of downstream privacy threats, such as re-identification, attribute inference, profiling or membership inference, can be carried out with significantly higher success rates. As such, reconstruction risk serves as a powerful proxy for broader privacy leakage, making it a natural privacy criterion and more interpretable than  $\varepsilon$ .
- **Utility**, measured as the variance (*i.e.*, MSE) in frequency estimation, which directly quantifies the deviation between true and estimated statistics and is central in frequency estimation tasks [22], [30], [31]. Moreover, minimizing MSE inherently reduces other utility losses such as MAE and Fisher Information loss [32] through established theoretical relationships like the Central Limit Theorem and Cramér-Rao bounds [40]–[42].

This ASR-MSE formulation captures a critical privacy-utility frontier that is central to many LDP deployments, and both metrics admit closed-form expressions for a wide range of protocols (see Section IV).

### C. Protocol Selection via Pareto Optimization

Given that ASR and MSE represent competing objectives, we search for **Pareto-efficient configurations** of protocol parameters. To this end, we first evaluate the objective metrics across a predefined parameter grid [43] to construct the

Pareto frontier. Then, to select a concrete operating point on this frontier, we consider several established multi-objective selection strategies [44]:

- **Utopia Point Minimization**, which picks the solution closest to the ideal point (ASR = 0, MSE = 0);
- **Weighted Scalarization**, which minimizes a linear combination of ASR and MSE via tunable weights;
- **Elbow (Knee) Method**, which identifies the point of maximum curvature on the frontier;
- **$\epsilon$ -Constraint Selection**, which filters solutions with ASR  $\leq \epsilon$  and then picks the one with minimum MSE (we default it back to utopia if no feasible point exists);
- **Hypervolume Contribution**, which selects the Pareto point contributing the largest area (in 2D) to the dominated space relative to a reference point (e.g., (1,1)), thereby improving coverage of the frontier;
- **Augmented Tchebycheff Scalarization**, which selects the point minimizing  $\max_i \{w_i f_i\} + \rho \sum_i w_i f_i$ , emphasizing worst-case performance while regularizing toward balanced objectives.

Among these, **weighted scalarization** stands out as a practical default due to its conceptual simplicity, interpretability and tunable nature. Empirically, we observed that all selection methods, except for the Elbow and  $\epsilon$ -Constraint methods, tend to identify similar parameters (see Figure 9 in Appendix B). Therefore, while our framework and implementation support multiple optimization criteria, we adopt weighted scalarization as the default approach for selecting protocol parameters:

$$\begin{aligned} \min_{\Theta} \quad & J(\Theta) = w_{\text{ASR}} \cdot \mathbb{E}[\text{ASR}] + w_{\text{MSE}} \cdot \text{MSE}, \\ \text{s.t.} \quad & w_{\text{ASR}} + w_{\text{MSE}} = 1. \end{aligned} \quad (23)$$

The weight  $w_{\text{ASR}}$  and  $w_{\text{MSE}}$  in Equation (23) can be tuned depending on the context. This flexibility enables LDP deployments to be tailored to different risk-utility trade-offs, enhancing applicability across diverse real-world scenarios. For privacy-critical applications, increasing  $w_{\text{ASR}}$  yields safer mechanisms while for analytics-heavy settings, higher  $w_{\text{MSE}}$  emphasizes utility. Importantly, setting  $w_{\text{MSE}} = 1$  recovers the original protocols, showing that **our refined mechanisms generalize rather than replace** their classical counterparts.

#### D. Adaptive Parameter Optimization for LDP Protocols

Using our two-objective framework defined in Equation (23), we extend four state-of-the-art LDP protocols to introduce adaptive counterparts. Each adaptive protocol selects an optimal parameter  $\Theta$  to achieve a better trade-off between ASR and MSE, rather than focusing solely on utility. The optimization process varies across protocols, adapting their internal parameters to balance privacy protection and estimation accuracy. **Importantly, our reparametrization preserves the original  $\epsilon$ -LDP guarantee by design. For instance, the subset size  $\omega$  in ASS and the probability pair  $(p, q)$  in AUE are explicitly constrained to satisfy the  $\epsilon$ -LDP guarantee; ALH inherits the privacy guarantee of GRR applied to a hashed domain; and ATHE applies a post-processing threshold, which does not affect the privacy guarantee.**

1) **Adaptive Subset Selection (ASS)**: The ASS mechanism extends the SS protocol. Unlike SS, which aims to minimize the estimation error alone when selecting  $\omega$ , ASS jointly optimizes it for both MSE and ASR. Formally, the optimization problem for ASS is defined as:

$$\begin{aligned} \min_{\omega \in \mathbb{Z}} \quad & J(\omega) = w_{\text{MSE}} \cdot \left( \frac{(k-1)(k+2\omega e^\epsilon - \omega)}{n\omega(-k+\omega+(k-1)e^\epsilon - (\omega-1)e^\epsilon)^2} \right. \\ & \left. + \frac{(k-\omega+(\omega-1)e^\epsilon)(-\omega(k-\omega)-\omega(\omega-1)e^\epsilon)}{n\omega(-k+\omega+(k-1)e^\epsilon - (\omega-1)e^\epsilon)^2} \right) \\ & + w_{\text{ASR}} \cdot \left( \frac{e^\epsilon}{\omega e^\epsilon + k - \omega} \right), \\ \text{s.t.} \quad & 1 \leq \omega < k, \quad w_{\text{ASR}} + w_{\text{MSE}} = 1. \end{aligned} \quad (24)$$

The range  $1 \leq \omega < k$  ensures that at least one value is selected while keeping the subset smaller than the total domain size. This prevents trivial cases where  $\omega = k$  would result in full randomness in the response or  $\omega = 0$  (no report).

2) **Adaptive Unary Encoding (AUE)**: The AUE mechanism is a generalization of UE protocols. Unlike the optimized UE protocol (i.e., OUE [22]), which only aims to minimize the estimation error setting a fixed  $p = 1/2$  and  $q = \frac{1}{e^\epsilon + 1}$ , AUE jointly optimizes both MSE and ASR by adapting the probabilities  $p$  and  $q$ . Formally, the optimization problem for AUE is defined as:

$$\begin{aligned} \min_{p \in \mathbb{R}} \quad & J(p) = w_{\text{MSE}} \cdot \left( \frac{((e^\epsilon - 1)q + 1)^2}{n(e^\epsilon - 1)^2(1-q)q} \right) \\ & + w_{\text{ASR}} \cdot \left( (1-p)(1-q)^{k-1} \cdot \frac{1}{k} \right. \\ & \left. + \sum_{m=1}^k p \cdot \frac{1}{m} \cdot \binom{k-1}{m-1} q^{m-1} (1-q)^{(k-1)-(m-1)} \right), \\ \text{s.t.} \quad & 0.5 \leq p < 1, \quad q = \frac{p}{e^\epsilon(1-p) + p}, \quad w_{\text{ASR}} + w_{\text{MSE}} = 1. \end{aligned} \quad (25)$$

The equality constraint for  $q$  is due to the  $\epsilon$ -LDP requirement for UE protocols:  $\epsilon = \ln \left( \frac{p(1-q)}{(1-p)q} \right)$  [3], [22].

3) **Adaptive LH (ALH)**: The ALH mechanism extends the LH protocol. Unlike the optimized LH protocol (i.e., OLH [22]), which aims solely to minimize estimation error by selecting  $g = \lfloor e^\epsilon + 1 \rfloor$ , ALH jointly optimizes both MSE and ASR by adapting the hash domain size parameter  $g$ . Formally, the optimization problem for ALH is defined as:

$$\begin{aligned} \min_{g \in \mathbb{Z}} \quad & J(g) = w_{\text{MSE}} \cdot \left( \frac{(e^\epsilon - 1 + g)^2}{n(e^\epsilon - 1)^2(g-1)} \right) \\ & + w_{\text{ASR}} \cdot \left( \frac{e^\epsilon}{(e^\epsilon + g - 1) \cdot \max \left\{ \frac{k}{g}, 1 \right\}} \right), \\ \text{s.t.} \quad & 2 \leq g \leq \max(k, \lfloor e^\epsilon + 1 \rfloor), \quad w_{\text{ASR}} + w_{\text{MSE}} = 1, \end{aligned} \quad (26)$$

The upper bound for  $g$  is set to  $\max(k, \lfloor e^\epsilon + 1 \rfloor)$ , ensuring that  $g$  is not unnecessarily smaller than the original domain size  $k$ . This avoids under-hashing, allowing for better differentiation and randomness. When  $k$  is large,  $g$  should ideally

match or exceed  $k$ , ensuring that hashing effectively introduces randomness to maintain privacy guarantees.

4) **Adaptive THE (ATHE)**: The ATHE mechanism extends the THE protocol. Unlike THE [22], which only aims to minimize the MSE in Equation (20), ATHE jointly optimizes both MSE and ASR by adapting the threshold parameter  $\theta$ . Formally, the optimization problem for ATHE is defined as:

$$\begin{aligned} \min_{\theta \in \mathbb{R}} \quad & J(\theta) = w_{\text{MSE}} \cdot \left( \frac{2e^{\varepsilon\theta/2} - 1}{n(1 + e^{\varepsilon(\theta-1/2)} - 2e^{\varepsilon\theta/2})^2} \right) \\ & + w_{\text{ASR}} \cdot \left( (1-p)(1-q)^{k-1} \cdot \frac{1}{k} + \frac{p}{kq} (1 - (1-q)^k) \right), \\ \text{s.t.} \quad & 0.5 \leq \theta \leq 1, \quad w_{\text{ASR}} + w_{\text{MSE}} = 1, \end{aligned} \quad (27)$$

in which  $p$  and  $q$  are given in Equation (18). The constraint  $0.5 \leq \theta \leq 1$  follows the settings used in prior work [22].

## VI. EXPERIMENTS AND ANALYSIS

The objective of our experiments is to thoroughly evaluate the performance of the proposed adaptive LDP protocols in terms of privacy, utility and resilience against data reconstruction attacks. Specifically, in Section VI-B, we conduct an **ASR analysis** for each LDP protocol to quantify their vulnerability to data reconstruction attacks, thereby assessing the privacy guarantees offered by existing and newly proposed mechanisms. Subsequently, in Section VI-C, we perform an **MSE analysis** to evaluate the utility guarantees provided by existing and our newly proposed mechanisms. Next, in Section VI-D, we explore the **trade-off between ASR and MSE** (*i.e.*, Pareto frontier), highlighting how our adaptive protocols compare to traditional ones in balancing privacy and utility under different scenarios. We then assess in Section VI-E the **impact of different weights**  $w_{\text{ASR}}$  and  $w_{\text{MSE}}$  in the objective function to provide insights into the influence of prioritizing privacy versus utility. Afterwards, we briefly analyze in Section VI-F the **parameter optimization** approach for each adaptive protocol.

We highlight that to systematize these aforementioned experiments, we rely primarily on the **analytical closed-form equations** for both MSE and ASR, as prior research has demonstrated a strong agreement between analytical and empirical results [12], [22], [28]. This choice allows us to comprehensively evaluate the performance of our protocols across a wide range of scenarios while avoiding computational overhead. Nonetheless, we also include a concise **empirical validation** in Section VI-G and Appendix D to ensure consistency and reinforce the validity of our analytical findings.

### A. Setup of Analytical Experiments

For all experiments, we have used the following settings:

- **Environment.** All algorithms are implemented in Python 3 and run on a desktop machine with 3.2GHz Intel Core i9 and 64GB RAM. All our code will be open-sourced.
- **LDP protocols.** We experiment with the eight LDP protocols described in Section IV and our four adaptive LDP protocols described in Section V-D.

- **Number of users.** For the analytical variance/MSE derived from Equation (4) (*e.g.*, Equation (6) for GRR, Equation (20) for THE, ...), we report variance per user, corresponding to the analytical derivation of  $\text{Var}[\cdot]/n$ . This allows us to examine the fundamental properties of each protocol independently of the dataset size.
- **Privacy parameter.** The LDP frequency estimation protocols were evaluated under two privacy regimes:
  - a) **High privacy regime** with  $\varepsilon \in \{0.5, 0.6, \dots, 1.9, 2.0\}$ .
  - b) **Medium to low privacy regime** with  $\varepsilon \in \{2.0, 2.5, \dots, 9.5, 10.0\}$ .
- **Domain size.** We vary the domain size in three ranges:
  - a) **Small domain:**  $k \in \{25, 50, 75, 100\}$ .
  - b) **Medium domain:**  $k \in \{250, 500, 750, 1000\}$ .
  - c) **Large domain:**  $k \in \{2500, 5000, 7500, 10000\}$ .
- **Weights for optimization.** Unless otherwise mentioned, we fix the weights for the two-objective optimization to  $w_{\text{ASR}} = w_{\text{MSE}} = 0.5$ , aiming for a balanced trade-off between privacy and accuracy. Experiments in Section VI-E will focus on varying these weights.
- **Optimization method.** Parameters for our adaptive protocols (*e.g.*, subset size  $\omega$  for ASS) were tuned via grid search [43], followed by selection using a *Weighted Scalarization* strategy (see Section V-C). While grid search is exhaustive and ensures broad coverage of the parameter space, it can be computationally expensive. For large or high-dimensional search spaces, we recommend constrained or gradient-free optimization methods [45] as a more efficient alternative to accelerate convergence without significantly sacrificing solution quality.

### B. ASR Analysis for LDP Protocols

In Figure 2, we evaluate the ASR for various LDP frequency estimation protocols as a function of the privacy budget  $\varepsilon$  from high to low privacy regimes across small to big domain sizes  $k$ . The goal of this analysis is to assess the robustness of each protocol against adversarial inference attacks under varying privacy levels and domain sizes. Specifically, we compare state-of-the-art protocols (GRR, SUE, BLH, OUE, OLH, SS, SHE and THE) against our proposed adaptive protocols (ASS, AUE, ALH and ATHE) to understand how effective these methods are at balancing privacy and utility.

**General trend across protocols:** For all protocols, we observe that the ASR generally increases with increasing privacy budget  $\varepsilon$  in Figure 2. This behavior is expected, as higher values of  $\varepsilon$  correspond to weaker privacy guarantees, allowing the adversary to infer user data more effectively. For smaller domain sizes (*i.e.*,  $k \leq 100$ ), the ASR rises sharply, suggesting that the adversary’s ability to correctly guess the user’s input improves significantly as  $\varepsilon$  increases. In contrast, larger domain sizes (*i.e.*,  $k \geq 1000$ ) show a more gradual increase in ASR, indicating that a larger domain inherently offers greater privacy protection. Nevertheless, **our adaptive methods effectively counteract privacy threats regardless of**

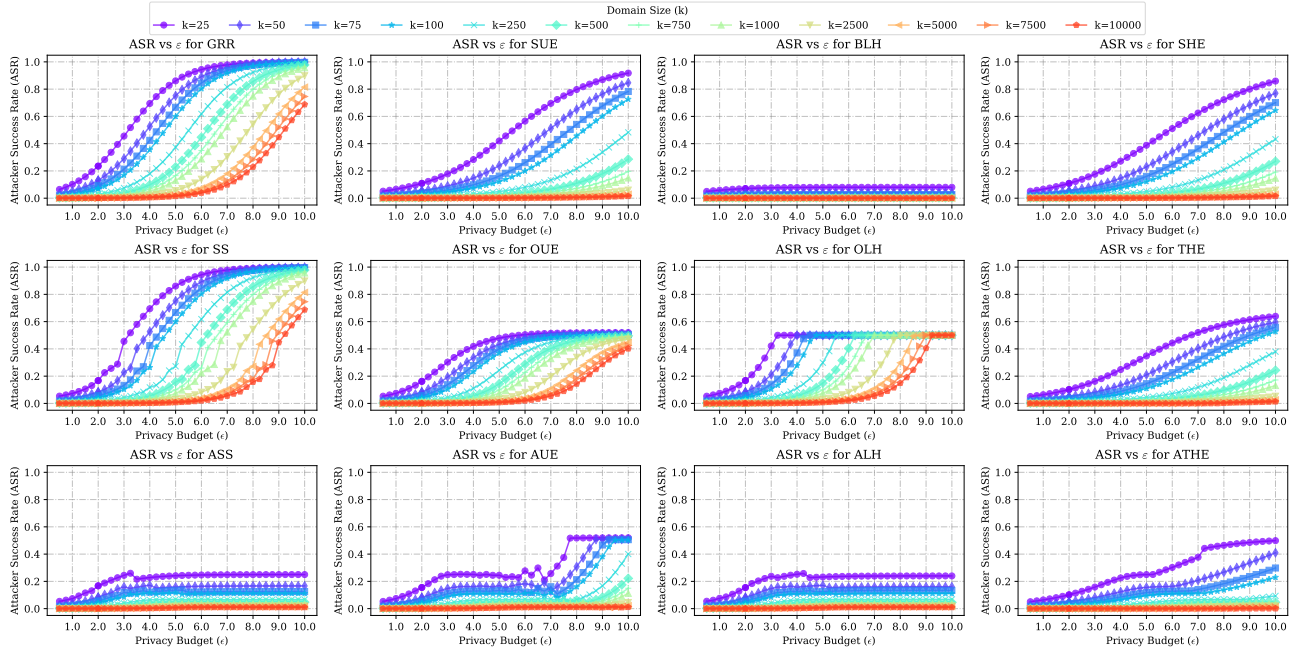


Fig. 2: Attacker Success Rate (ASR) vs. privacy budget ( $\epsilon$ ) for different LDP frequency estimation protocols across varying domain sizes ( $k$ ). The plots compare state-of-the-art LDP protocols, including GRR, SUE, BLH, OUE, OLH, SS, SHE and THE, against our newly proposed adaptive protocols (ASS, AUE, ALH and ATHE). Each curve represents a different domain size, with  $k$  ranging from 25 to 10000. The figure highlights the trade-offs between privacy and adversarial resilience for each protocol, showing how ASR evolves as the privacy budget and domain size change.

$k$  and  $\epsilon$ , underscoring the flexibility and robustness offered by our double-objective optimization framework.

**Comparing traditional protocols:** Among traditional protocols, GRR and SS demonstrate the highest ASR across all privacy budgets and domain sizes, making them the most vulnerable to privacy attacks. In contrast, SUE displays a more gradual increase in ASR, suggesting better resilience than GRR and SS. Protocols such as OUE and OLH exhibit a maximum ASR of approximately 0.5, even as  $\epsilon$  increases, showing a clear boundary in their ASR. Notably, for SHE, ASR grows gradually as  $\epsilon$  increases, while THE’s thresholding strategy yields moderate ASR increments. Overall, BLH consistently achieves an exceptionally low ASR across all privacy budgets and domain sizes, highlighting its robustness against adversarial inference attacks.

**Our refined and adaptive protocols:** Our adaptive protocols (*i.e.*, ASS, AUE, ALH and ATHE) demonstrate significantly lower ASR compared to their traditional counterparts across all privacy budgets. For example, ASS effectively mitigates the ASR vulnerability of the state-of-the-art SS by capping the ASR below 0.25, in contrast to the traditional SS where the ASR gets to 1 (*i.e.*, the adversary can fully infer the user’s value). Similarly, AUE consistently achieves a lower or comparable ASR relative to the state-of-the-art OUE protocol, highlighting the benefits of its adaptive parameter optimization. For ALH, the adaptive mechanism achieves a balanced compromise between the low ASR of BLH and the moderate ASR of OLH by dynamically optimizing the

hash domain size, resulting in a substantial reduction in ASR compared to traditional OLH. Finally, ATHE demonstrates more resilience than THE across all domain sizes, thereby showcasing the effectiveness of our framework in enhancing privacy protection.

**ASR increases with  $\epsilon$ , but our adaptive protocols resist:** As the privacy budget  $\epsilon$  increases, ASR generally rises for all protocols due to weaker privacy guarantees. However, our adaptive protocols (ASS, AUE, ALH and ATHE) exhibit significantly lower (*i.e.*,  $\leq 5$  orders of magnitude) ASRs across a broad range of  $\epsilon$  values, underscoring their enhanced resilience against privacy attacks and their ability to maintain robust privacy protection.

### C. MSE Analysis for LDP Protocols

In Figure 3, we examine the MSE behavior of UE-, LH- and HE-based LDP protocols, including our adaptive versions (AUE, ALH and ATHE) across varying privacy budgets  $\epsilon$ . In Figure 4, we extend this analysis to compare MSE trends for the SS protocol and its adaptive counterpart ASS. These analyses aim to determine whether the adaptive protocols’ improved robustness to privacy attacks results in substantial estimation accuracy loss or if they maintain competitive MSE values. Notice that the MSE curves of SUE, OUE, BLH, OLH, SHE and THE remain independent of the domain size  $k$  due to their fixed parameterization, as established in previous literature [22].

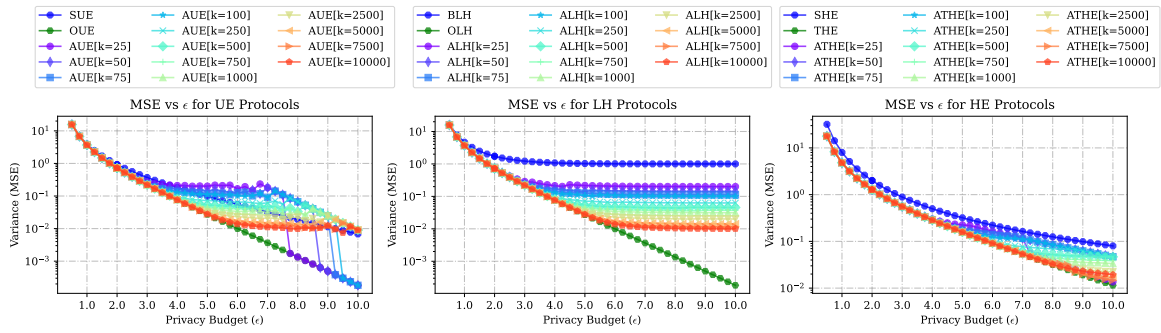


Fig. 3: Variance (MSE) vs. privacy budget ( $\epsilon$ ) for the state-of-the-art LDP protocols (UE-, LH-, and HE-based) and our adaptive versions (AUE, ALH, and ATHE) across various domain sizes  $k$ . For our adaptive protocols, each curve represents a distinct domain size, illustrating how each protocol balances estimation accuracy with privacy as  $\epsilon$  changes.

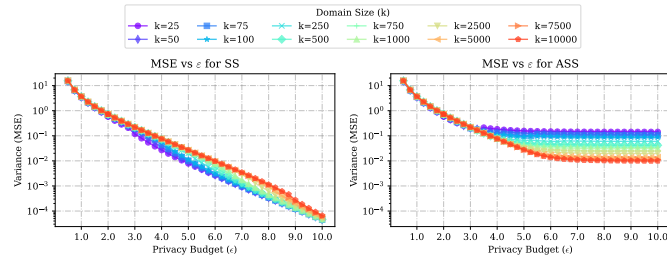


Fig. 4: Variance (MSE) vs. privacy budget ( $\epsilon$ ) for the state-of-the-art SS protocol and our adaptive version ASS across various domain sizes  $k$ . Each curve represents a distinct domain size, illustrating how each protocol balances estimation accuracy with privacy as  $\epsilon$  changes.

For the SS protocol, we observe in Figure 4 that ASS exhibits an increase in MSE by up to two orders of magnitude compared to SS, particularly in higher privacy regimes ( $\epsilon \geq 4$ ). This increase is expected, as SS’s minimal MSE comes at the cost of extreme vulnerability, with ASR approaching 1 (e.g., see Figure 2), meaning an adversary can fully infer the user’s value. ASS, in contrast, balances this trade-off by introducing adaptive parameterization that mitigates privacy attacks while moderately increasing the MSE.

In Figure 3, we observe similar trends for the other adaptive protocols (AUE, ALH, and ATHE). For UE protocols, our adaptive AUE version achieves slightly higher MSE compared to OUE across all domain sizes  $k$ , with the gap becoming more pronounced as  $\epsilon$  increases. This is expected, as AUE optimizes its parameters to enhance robustness to privacy attacks, leading to a slight trade-off in utility. Notably, AUE remains competitive with SUE in high privacy regimes ( $\epsilon \leq 2$ ), offering similar MSE levels while achieving significantly improved ASR performance as shown earlier. In low privacy regimes ( $\epsilon > 2$ ), AUE incurs a modest increase in MSE, which stays within an order of magnitude compared to OUE.

Moreover, for LH- and HE-based protocols, we observe in Figure 3 that our adaptive protocols (ALH and ATHE) demonstrate a variance (MSE) behavior that is consistently

“sandwiched” between the two corresponding state-of-the-art protocols in their respective groups. Specifically, ALH achieves MSE values between those of BLH (which minimizes ASR at the cost of higher MSE) and OLH (which minimizes MSE but is more vulnerable to privacy attacks). Similarly, ATHE’s variance lies between SHE and THE, showing a trade-off where ATHE retains competitive MSE while prioritizing adversarial resilience. This positioning highlights how adaptivity allows our protocols to achieve a better privacy-utility trade-off.

**Adaptive protocols maintain competitive MSE:** Our adaptive protocols (ASS, AUE, ALH and ATHE) achieve higher MSE compared to their non-adaptive counterparts. However, these increases remain within acceptable bounds ( $\leq 2$  orders of magnitude), highlighting that the improved adversarial resilience ( $\text{ASR} \leq 5$  orders of magnitude) comes at a reasonable cost to the utility. This suggests that enhanced privacy protection against adversaries can be achieved without prohibitive increases in variance.

#### D. Pareto Frontier for ASR and MSE

In addition to evaluating how the ASR and the MSE vary with the privacy budget  $\epsilon$  separately (see Figures 2, 4 and 3), it is insightful to examine how ASR changes as a function of utility loss, measured by the variance (MSE) of the frequency estimation. Figure 5 presents the Pareto frontier between ASR and MSE for the considered LDP protocols, plotting ASR against MSE across small domain sizes and medium to low privacy regimes. This analysis highlights the performance of state-of-the-art protocols (GRR, SUE, BLH, SHE, SS, OUE, OLH and THE) compared to our adaptive variants (ASS, AUE, ALH and ATHE), providing insights into how effectively each method navigates the trade-off between user privacy and data utility. To address space limitations, additional results exploring the ASR-MSE trade-off under varying privacy regimes (high, medium, low) and domain sizes (small, medium, large) are provided in Appendix C. The findings and discussions in this section are supported by a comprehensive analysis that includes these extended results.

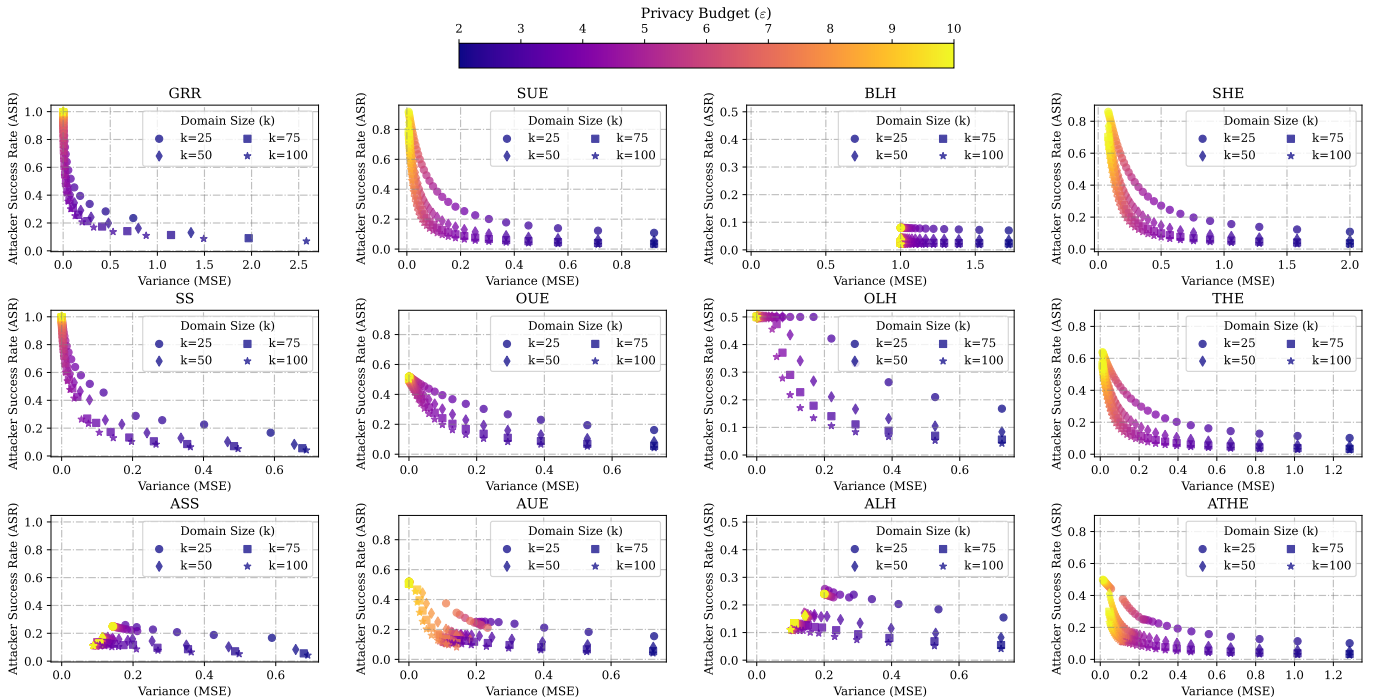


Fig. 5: Attacker Success Rate (ASR) vs. Variance (MSE) for numerous LDP frequency estimation protocols. Each plot shows how each protocol performs under varying privacy budgets  $\epsilon$  and domain sizes ( $k$ ), illustrating the trade-off between adversarial success rate (ASR) and utility (MSE). State-of-the-art LDP protocols (*i.e.*, GRR, SUE, BLH, SHE, SS, OUE, OLH and THE) are compared against our adaptive counterparts (*i.e.*, ASS, AUE, ALH and ATHE). Each point represents a different configuration of  $\epsilon$  (in medium to low privacy regimes) and  $k$  (small domain), with colors indicating the privacy budget level.

**General trend across protocols:** For all protocols, there is a clear inverse relationship between ASR and MSE – lower variance estimates correspond to higher ASR, and vice versa. As the privacy budget  $\epsilon$  increases, protocols tend to yield estimates with lower MSE but simultaneously face higher ASRs, reflecting a direct cost to privacy when pursuing higher accuracy. Conversely, under stricter privacy regimes (lower  $\epsilon$ ), while ASR remains lower, the resulting estimates incur greater MSE. This fundamental tension highlights that simply tuning  $\epsilon$  does not guarantee a balanced privacy-utility outcome. Thus, understanding the ASR-MSE relationship is crucial for informed protocol selection.

**Comparing traditional protocols:** Among the traditional protocols, GRR and SS tend to cluster in regions with relatively lower MSE but higher ASR, especially at moderate-to-high  $\epsilon$  values. In contrast, SUE, SHE, and THE provide a more gradual trade-off curve, achieving lower ASR at slightly higher MSE levels, suggesting that these methods preserve more privacy when aiming for moderate accuracy. OUE and OLH occupy intermediate positions: they can reach points of low MSE but at the cost of increasing  $\epsilon$ . BLH generally exhibits a low ASR while not bounding the MSE, indicating a low privacy-utility trade-off. Overall, none of the traditional protocols dominate the entire ASR-MSE space, and their effectiveness varies with the chosen privacy budget and domain size.

**Our refined and adaptive protocols:** Our adaptive protocols achieve more favorable ASR-MSE trade-offs, especially providing low-ASR even in low-privacy regimes (*i.e.*, high  $\epsilon$  values). For instance, ASS, derived from SS, effectively prevents the sharp ASR increases observed in SS’s low-MSE regions by fine-tuning protocol parameters, resulting in points that align closer to a Pareto frontier between ASR and MSE. AUE, adapting from OUE, displays a particularly strong trade-off, often settling into low-ASR regimes without disproportionately large MSE. ALH, building on hashing-based approaches, maintains ASR reductions comparable to BLH or OLH but achieves them with more controlled MSE levels, ensuring that the benefits of hashing-based schemes are not compromised. ATHE consistently achieves configurations that lower ASR without excessively increasing MSE, indicating a more harmonious balance.

**ASR-MSE trade-offs are protocol-dependent:** Our findings show that each protocol exhibits a distinct ASR-MSE profile. By jointly optimizing for both ASR and MSE, our adaptive protocols consistently push these curves toward more favorable regimes in the ASR-MSE Pareto frontier.

#### E. Impact of Weights in the Objective Function

Thus far, we have focused on analyzing the performance of adaptive protocols under fixed objective configurations for the weights ( $w_{ASR} = w_{MSE} = 0.5$ ) in Equation (23). However, our

proposed multi-objective framework introduces a new degree of freedom: practitioners can adjust the relative importance of ASR vs. variance (MSE) when optimizing LDP protocols. Figure 6 illustrates how varying these weight combinations ( $w_{ASR}, w_{MSE}$ ) influences the ASR, MSE, and optimal parameter choices for AUE ( $p$ ), ALH ( $g$ ), ASS ( $\omega$ ) and ATHE ( $\theta$ ) under a fixed setting ( $k = 100, \varepsilon = 4$ ).

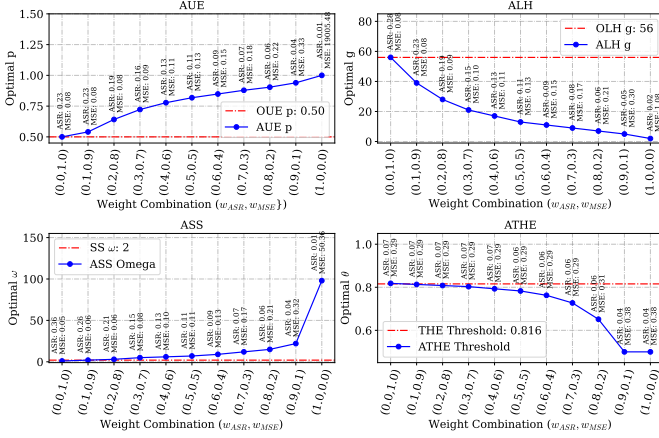


Fig. 6: Optimal parameter choices for each adaptive protocol as a function of the weight combination ( $w_{ASR}, w_{MSE}$ ), evaluated at  $k = 100$  and  $\varepsilon = 4$ . Each sub-figure compares the adaptive protocol’s chosen parameter (blue color curve) against the corresponding parameter choice in the original, non-adaptive protocol (red color dashed line).

From Figure 6, one can notice that as the weight on ASR  $w_{ASR}$  increases, each adaptive protocol tends to choose parameter values that more aggressively reduce the ASR at the cost of increasing the MSE. Conversely, placing greater emphasis on MSE drives parameters toward configurations closer to or equal to those of the original protocols (*i.e.*, SS, OUE, OLH and THE), aiming to preserve utility even if it elevates the ASR. These results confirm the benefits of our two-objective optimization framework: rather than a static parameter choice, practitioners can tune the protocol parameters in response to changing priorities, achieving a more flexible trade-off between privacy (ASR) and utility (MSE).

### F. Adaptive and Optimized Parameters

In this section, we analyze the optimization of parameters in our adaptive protocols (AUE, ALH, ASS and ATHE) by examining the behavior of their objective functions (Equations (24)–(27)), which balance the ASR-MSE trade-off. Figure 7 illustrates the objective function as a function of key parameters: AUE ( $p$ ), ALH ( $g$ ), ASS ( $\omega$ ) and ATHE ( $\theta$ ), with a fixed  $k = 100$  and  $\varepsilon = 4$ . The selected parameters for our adaptive protocols are compared against the fixed state-of-the-art parameters of OUE, OLH, SS and THE.

For **AUE**, we observe in the top-left plot that the objective function reaches its minimum at  $p = 0.818$ , which is notably higher than the fixed  $p = 0.5$  used by OUE. This also means that parameter  $q$  will increase to satisfy  $\varepsilon$ -LDP, *i.e.*,

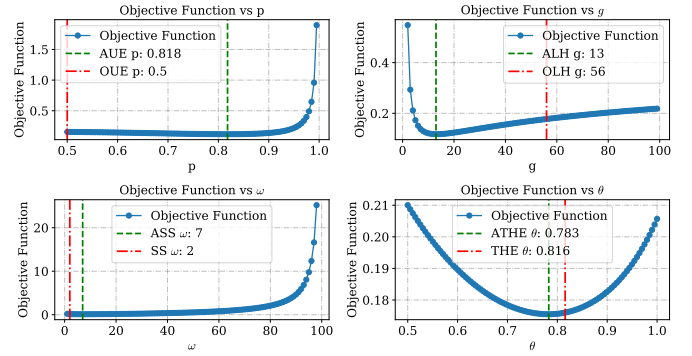


Fig. 7: Objective function value as a function of key parameters for our adaptive protocols (AUE, ALH, ASS and ATHE) compared with their state-of-the-art counterparts (OUE, OLH, SS and THE). Vertical dashed lines (green color) indicate the optimal parameter values selected by our adaptive protocols, while vertical dash-dotted lines (red color) represent the fixed parameter values of the state-of-the-art protocols. Without loss of generality, we set  $k = 100$  and  $\varepsilon = 4$ .

increasing the probability of reporting random bits. For **ALH**, as shown in the top-right plot, the optimal hash domain size is reduced to  $g = 13$  in our adaptive protocol compared to  $g = 56$  in OLH. This reduction in  $g$  lowers the ASR at the expense of slightly increased variance, aligning with our adaptive objective to achieve a better balance between privacy and utility. For **ASS**, as depicted in the bottom-left plot, the optimal subset size  $\omega = 7$  contrasts with the fixed  $\omega = 2$  used in SS. The larger  $\omega$  effectively spreads the probability mass across a larger subset, reducing ASR while incurring a higher variance. For **ATHE**, the bottom-right plot shows that the adaptive threshold  $\theta = 0.783$  is slightly lower than the fixed threshold  $\theta = 0.816$  in THE. This subtle adjustment enables ATHE to reduce privacy attacks while maintaining competitive variance levels, showcasing the precision of our adaptive optimization.

**Adaptive protocols optimize parameters for better trade-offs:** Our findings demonstrate that the optimized parameters selected by adaptive protocols significantly differ from the fixed parameters of state-of-the-art protocols, resulting in improved robustness to privacy attacks with controlled increases in variance. This optimization highlights the effectiveness of our adaptive mechanisms in better navigating the privacy-utility trade-off space.

### G. Empirical Pareto Frontier for ASR and MSE

To assess the accuracy of our closed-form ASR and MSE equations within the ASR-MSE two-objective framework (Section V-B), we conduct empirical experiments using the **Adult** dataset from the UCI machine learning repository [46]. We select the Age attribute with domain size  $k = 100$  (*i.e.*, Age  $\in [0, 99]$ ) and  $n = 48842$  users, reporting results averaged over 100 independent runs.

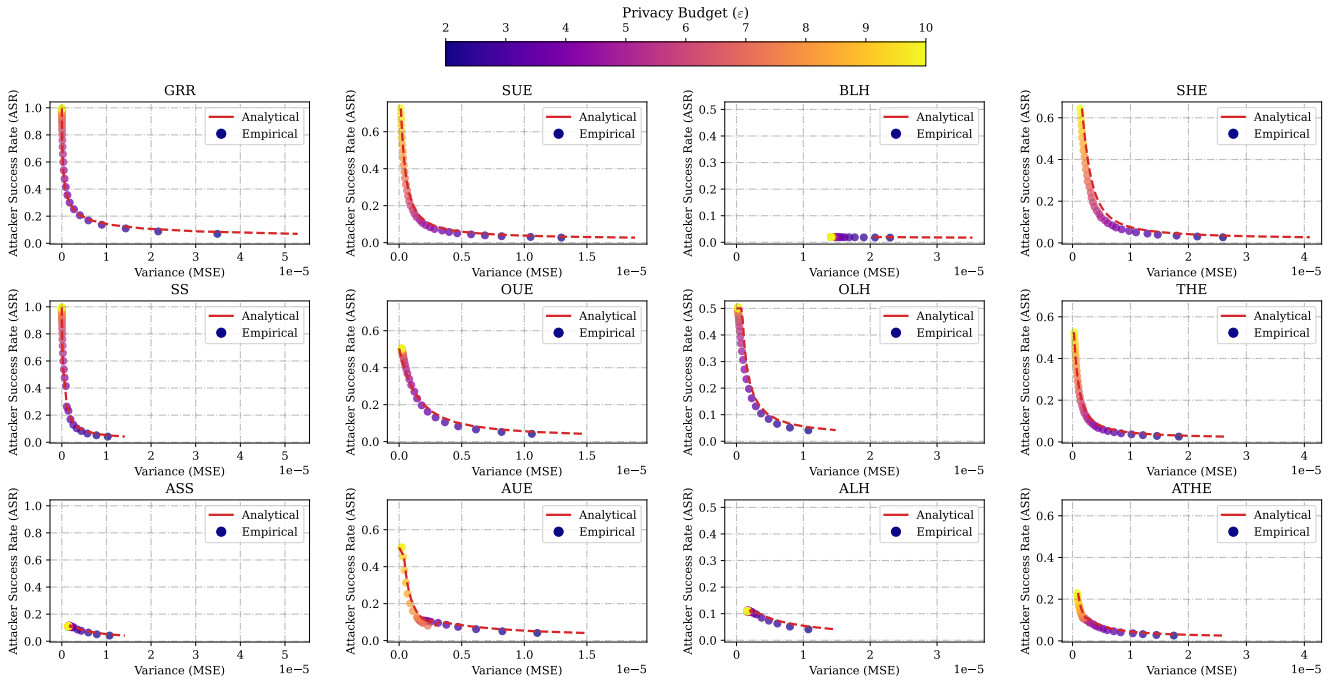


Fig. 8: Comparison of empirical and analytical Pareto frontiers for ASR vs. Variance (MSE) across various LDP protocols (state-of-the-art and adaptive). Each subplot considers a range of privacy budgets  $\epsilon \in (2, 10)$  and a fixed domain size  $k = 100$ . Empirical results ( $\circ$  markers) are averaged over 100 independent runs with the `Age` attribute of the Adult dataset [46], while analytical results (red dashed lines) are computed using closed-form equations.

Figure 8 presents the comparison between **empirical** ( $\circ$  markers) and **analytical** (red dashed lines) Pareto frontiers for ASR versus MSE across various LDP protocols, including both state-of-the-art and our adaptive variants. Each subplot represents a specific protocol (*i.e.*, GRR, SUE, BLH, SHE, SS, OUE, OLH, THE, ASS, AUE, ALH and ATHE) with the privacy budget varying as  $\epsilon \in (2, 10)$  with the domain size fixed at  $k = 100$ . One can notice that across all protocols, the empirical results closely align with the analytical calculation, showcasing the robustness of the closed-form equations for ASR and MSE. This alignment highlights the reliability of our theoretical framework and previous analytical experiments across different privacy budgets and data distributions. To further support this claim, similar to Figure 1, Appendix D provides additional experiments using a synthetic dataset generated from a Dirichlet distribution (1), exploring variations in the number of users ( $n \in \{5000, 50000, 500000\}$ ).

**Analytical vs. empirical validation:** Our findings demonstrate that the analytical results closely align with empirical ones, reaffirming the reliability of the closed-form equations across various privacy budgets and scenarios.

## VII. CONCLUSION AND PERSPECTIVES

In this work, we introduced a **general multi-objective optimization framework** for refining LDP frequency estimation protocols under adversarial conditions. Unlike prior approaches that minimize estimation error (MSE) in iso-

lation, our framework allows for principled, flexible trade-offs between utility and privacy, selecting protocol parameters through classical multi-objective optimization strategies while strictly preserving the original  $\epsilon$ -LDP guarantees. As an instantiation of this framework, we focused on a two-objective formulation that jointly minimizes the Attacker Success Rate (ASR) under *data reconstruction attacks* [26], [28], [29] and Mean Squared Error (MSE), demonstrating that existing protocols (*i.e.*, SS, OUE, OLH and THE) can be substantially improved through principled parameter tuning. Our adaptive protocols, namely, ASS, AUE, ALH and ATHE, can significantly reduce privacy leakage while maintaining high accuracy across a wide range of scenarios, making our methods directly applicable in real-world systems.

To our knowledge, this is the **first work to jointly optimize analytical ASR and MSE via flexible, selector-driven parameter tuning**, all while preserving  $\epsilon$ -LDP and extending analytical formulations to new protocols. This contribution bridges a gap between theoretical guarantees and practical deployment risks, offering a robust methodology to assess and mitigate vulnerabilities in LDP mechanisms. Looking ahead, our framework is extensible to broader privacy, utility, and security objectives, including robustness to poisoning [34], [36], resistance to inference [9], [27], [33] or re-identification attacks [25], [26], and even communication efficiency. Finally, we envision this work as a foundation for a modular LDP optimization suite, paving the way for adaptive, attack-aware LDP deployments at scale.

## ACKNOWLEDGMENT

This work has been partially supported by the French National Research Agency (ANR), under contract “ANR-24-CE23-6239” JCJC project AI-PULSE and by the “ANR 22-PECY-0002” IPOP (Interdisciplinary Project on Privacy) project of the Cybersecurity PEPR. Sébastien Gambs is supported by the Canada Research Chair program as well as a Discovery Grant from NSERC.

## REFERENCES

- [1] C. Dwork, F. McSherry, K. Nissim, and A. Smith, “Calibrating noise to sensitivity in private data analysis,” in *Theory of Cryptography*. Springer Berlin Heidelberg, 2006, pp. 265–284.
- [2] S. P. Kasiviswanathan, H. K. Lee, K. Nissim, S. Raskhodnikova, and A. Smith, “What can we learn privately?” *SIAM Journal on Computing*, vol. 40, no. 3, pp. 793–826, 2011.
- [3] U. Erlingsson, V. Pihur, and A. Korolova, “RAPPOR: Randomized aggregatable privacy-preserving ordinal response,” in *Proceedings of the 2014 ACM SIGSAC Conference on Computer and Communications Security*. New York, NY, USA: ACM, 2014, pp. 1054–1067.
- [4] B. Ding, J. Kulkarni, and S. Yekhanin, “Collecting telemetry data privately,” in *Advances in Neural Information Processing Systems 30*, I. Guyon, U. V. Luxburg, S. Bengio, H. Wallach, R. Fergus, S. Vishwanathan, and R. Garnett, Eds. Curran Associates, Inc., 2017, pp. 3571–3580.
- [5] R. Bassily and A. Smith, “Local, private, efficient protocols for succinct histograms,” in *Proceedings of the Forty-Seventh Annual ACM Symposium on Theory of Computing*, ser. STOC ’15. New York, NY, USA: Association for Computing Machinery, 2015, p. 127–135.
- [6] X. Li, W. Liu, J. Lou, Y. Hong, L. Zhang, Z. Qin, and K. Ren, “Local differentially private heavy hitter detection in data streams with bounded memory,” *Proc. ACM Manag. Data*, vol. 2, no. 1, Mar. 2024.
- [7] Y. Zhang, Q. Ye, and H. Hu, “Federated heavy hitter analytics with local differential privacy,” *Proc. ACM Manag. Data*, vol. 3, no. 1, Feb. 2025.
- [8] H. H. Arcolezi, J.-F. Couchot, B. A. Bouna, and X. Xiao, “Improving the utility of locally differentially private protocols for longitudinal and multidimensional frequency estimates,” *Digital Communications and Networks*, vol. 10, no. 2, pp. 369–379, 2024.
- [9] H. H. Arcolezi, C. A. Pinzón, C. Palamidessi, and S. Gambs, “Frequency estimation of evolving data under local differential privacy,” in *Proceedings of the 26th International Conference on Extending Database Technology, EDBT 2023, Ioannina, Greece, March 28 - March 31, 2023*. OpenProceedings.org, 2023, pp. 512–525.
- [10] X. Gu, M. Li, Y. Cao, and L. Xiong, “Supporting both range queries and frequency estimation with local differential privacy,” in *2019 IEEE Conference on Communications and Network Security (CNS)*, 2019, pp. 124–132.
- [11] J. Yang, T. Wang, N. Li, X. Cheng, and S. Su, “Answering multi-dimensional range queries under local differential privacy,” *arXiv preprint arXiv:2009.06538*, 2020.
- [12] H. H. Arcolezi, J.-F. Couchot, B. A. Bouna, and X. Xiao, “Random sampling plus fake data: Multidimensional frequency estimates with local differential privacy,” in *Proceedings of the 30th ACM International Conference on Information & Knowledge Management*. ACM, oct 2021, pp. 47–57.
- [13] J. S. Costa Filho and J. C. Machado, “Felip: A local differentially private approach to frequency estimation on multidimensional datasets,” in *Proceedings of the 26th International Conference on Extending Database Technology, EDBT 2023, Ioannina, Greece, March 28 - March 31, 2023*. OpenProceedings.org, 2023, pp. 671–683.
- [14] J. Li, W. Gan, Y. Gui, Y. Wu, and P. S. Yu, “Frequent itemset mining with local differential privacy,” in *Proceedings of the 31st ACM International Conference on Information & Knowledge Management*, ser. CIKM ’22. New York, NY, USA: Association for Computing Machinery, 2022, p. 1146–1155.
- [15] H. Wu, R. Ran, S. Peng, M. Yang, and T. Guo, “Mining frequent items from high-dimensional set-valued data under local differential privacy protection,” *Expert Systems with Applications*, vol. 234, p. 121105, Dec. 2023.
- [16] E. Alptekin and M. E. Gursoy, “Building quadrees for spatial data under local differential privacy,” in *IFIP Annual Conference on Data and Applications Security and Privacy*. Springer, 2023, pp. 22–39.
- [17] E. Tire and M. E. Gursoy, “Answering spatial density queries under local differential privacy,” *IEEE Internet of Things Journal*, vol. 11, no. 10, pp. 17419–17436, 2024.
- [18] R. Raab, P. Berrang, P. Gerhart, and D. Schröder, “Sok: Descriptive statistics under local differential privacy,” *Proceedings on Privacy Enhancing Technologies*, vol. 2025, no. 1, p. 118–149, Jan. 2025.
- [19] P. Kairouz, K. Bonawitz, and D. Ramage, “Discrete distribution estimation under local privacy,” in *International Conference on Machine Learning*. PMLR, 2016, pp. 2436–2444.
- [20] S. Wang, L. Huang, P. Wang, Y. Nie, H. Xu, W. Yang, X.-Y. Li, and C. Qiao, “Mutual information optimally local private discrete distribution estimation,” *arXiv preprint arXiv:1607.08025*, 2016.
- [21] M. Ye and A. Barg, “Optimal schemes for discrete distribution estimation under locally differential privacy,” *IEEE Transactions on Information Theory*, vol. 64, no. 8, pp. 5662–5676, 2018.
- [22] T. Wang, J. Blocki, N. Li, and S. Jha, “Locally differentially private protocols for frequency estimation,” in *26th USENIX Security Symposium (USENIX Security 17)*. Vancouver, BC: USENIX Association, Aug. 2017, pp. 729–745.
- [23] J. Acharya, Z. Sun, and H. Zhang, “Hadamard response: Estimating distributions privately, efficiently, and with little communication,” in *Proceedings of the Twenty-Second International Conference on Artificial Intelligence and Statistics*, ser. Proceedings of Machine Learning Research, K. Chaudhuri and M. Sugiyama, Eds., vol. 89. PMLR, 16–18 Apr 2019, pp. 1120–1129.
- [24] V. Feldman, J. Nelson, H. Nguyen, and K. Talwar, “Private frequency estimation via projective geometry,” in *Proceedings of the 39th International Conference on Machine Learning*, ser. Proceedings of Machine Learning Research, K. Chaudhuri, S. Jegelka, L. Song, C. Szepesvari, G. Niu, and S. Sabato, Eds., vol. 162. PMLR, 17–23 Jul 2022, pp. 6418–6433.
- [25] T. Murakami and K. Takahashi, “Toward evaluating re-identification risks in the local privacy model,” *Transactions on Data Privacy*, vol. 14, no. 3, pp. 79–116, 2021.
- [26] H. H. Arcolezi, S. Gambs, J.-F. Couchot, and C. Palamidessi, “On the risks of collecting multidimensional data under local differential privacy,” *Proc. VLDB Endow.*, vol. 16, no. 5, p. 1126–1139, jan 2023.
- [27] A. Gadotti, F. Houssiau, M. S. M. S. Annamalai, and Y.-A. de Montjoye, “Pool inference attacks on local differential privacy: Quantifying the privacy guarantees of apple’s count mean sketch in practice,” in *31st USENIX Security Symposium (USENIX Security 22)*. Boston, MA: USENIX Association, Aug. 2022, pp. 501–518.
- [28] M. Emre Gursoy, L. Liu, K.-H. Chow, S. Truex, and W. Wei, “An adversarial approach to protocol analysis and selection in local differential privacy,” *IEEE Transactions on Information Forensics and Security*, vol. 17, pp. 1785–1799, 2022.
- [29] H. H. Arcolezi and S. Gambs, “Revealing the true cost of locally differentially private protocols: An auditing perspective,” *Proceedings on Privacy Enhancing Technologies*, vol. 2024, no. 4, pp. 123–141, 2024.
- [30] Y. Wang, X. Wu, and D. Hu, “Using randomized response for differential privacy preserving data collection,” in *EDBT/ICDT Workshops*, vol. 1558, 2016, pp. 0090–6778.
- [31] G. Cormode, S. Maddock, and C. Maple, “Frequency estimation under local differential privacy,” *Proceedings of the VLDB Endowment*, vol. 14, no. 11, pp. 2046–2058, Jul. 2021.
- [32] L. P. Barnes, W.-N. Chen, and A. Özgür, “Fisher information under local differential privacy,” *IEEE Journal on Selected Areas in Information Theory*, vol. 1, no. 3, pp. 645–659, 2020.
- [33] M. E. GÜRSOY, “Longitudinal attacks against iterative data collection with local differential privacy,” *Turkish Journal of Electrical Engineering and Computer Sciences*, vol. 32, no. 1, p. 198–218, Feb. 2024.
- [34] X. Cao, J. Jia, and N. Z. Gong, “Data poisoning attacks to local differential privacy protocols,” in *30th USENIX Security Symposium (USENIX Security 21)*. USENIX Association, Aug. 2021, pp. 947–964.
- [35] S. L. Warner, “Randomized response: A survey technique for eliminating evasive answer bias,” *Journal of the American Statistical Association*, vol. 60, no. 309, pp. 63–69, Mar. 1965.
- [36] A. Cheu, A. Smith, and J. Ullman, “Manipulation attacks in local differential privacy,” in *2021 IEEE Symposium on Security and Privacy (SP)*. IEEE, May 2021.

- [37] I. Dinur and K. Nissim, "Revealing information while preserving privacy," in *Proceedings of the Twenty-Second ACM SIGMOD-SIGACT-SIGART Symposium on Principles of Database Systems*, ser. PODS '03. New York, NY, USA: Association for Computing Machinery, 2003, p. 202–210.
- [38] B. Balle, G. Cherubin, and J. Hayes, "Reconstructing training data with informed adversaries," in *2022 IEEE Symposium on Security and Privacy (SP)*, 2022, pp. 1138–1156.
- [39] P. Guerra-Balboa, A. Sauer, and T. Strufe, "Analysis and measurement of attack resilience of differential privacy," in *Proceedings of the 23rd Workshop on Privacy in the Electronic Society*, ser. WPES '24. New York, NY, USA: Association for Computing Machinery, 2024, p. 155–171.
- [40] C. R. Rao, "Information and the accuracy attainable in the estimation of statistical parameters," in *Breakthroughs in Statistics: Foundations and basic theory*. Springer, 1992, pp. 235–247.
- [41] H. Cramér, *Mathematical Methods of Statistics (PMS-9)*. Princeton University Press, 1999.
- [42] T. M. Cover and J. A. Thomas, *Elements of Information Theory (Wiley Series in Telecommunications and Signal Processing)*. USA: Wiley-Interscience, 2006.
- [43] J. Bergstra and Y. Bengio, "Random search for hyper-parameter optimization," *Journal of machine learning research*, vol. 13, no. 2, 2012.
- [44] R. F. Yezid Donoso, *Multi-Objective Optimization in Computer Networks Using Metaheuristics*, 1st ed. Auerbach Publications, 2007.
- [45] R. P. Brent, *Algorithms for minimization without derivatives*. Courier Corporation, 2013.
- [46] D. Dua and C. Graff, "UCI machine learning repository," 2017, available online: <http://archive.ics.uci.edu/ml>.

## APPENDIX

### A. Expected Data Reconstruction Attack Analyses

1) *UE Protocols*: Following the attack strategy for UE in Section IV-C, we consider two events:

- **Event 0**: The bit corresponding to the user's value  $x$  is flipped from 1 to 0, and all other bits remain 0.
  - The attacker's guess is uniformly distributed over all  $k$  possible values.
  - Success rate:  $\frac{1}{k}$ .
  - Probability:  $\Pr(\text{Event 0}) = (1-p)(1-q)^{k-1}$ .
- **Event 1**: The bit corresponding to the user's value  $x$  remains 1, and  $m-1$  of the remaining  $k-1$  bits are flipped from 0 to 1.
  - The attacker's guess is uniformly distributed over the bits set to 1.
  - If  $m$  bits are set to 1, the success rate is  $\frac{1}{m}$ .
  - Probability:  $\Pr(\text{Event 1 with } m \text{ bits set to 1}) = \binom{k-1}{m-1} p(q)^{m-1} (1-q)^{k-m}$ .

Thus, combining these two events, we can derive the expected ASR as:

$$\begin{aligned} \mathbb{E}[\text{ASR}]_{\text{UE}} &= \Pr(\text{Event 0}) \cdot \frac{1}{k} \\ &+ \sum_{m=1}^k \Pr(\text{Event 1 with } m \text{ bits set to 1}) \cdot \frac{1}{m}. \end{aligned}$$

More formally, the probability calculations of each event are:

#### 1) Probability of Event 0:

$$\Pr(\text{Event 0}) = (1-p)(1-q)^{k-1}.$$

#### 2) Probability of Event 1 with $m$ bits set to 1:

$$\begin{aligned} \Pr(\text{Event 1 with } m \text{ bits set to 1}) &= \\ &\binom{k-1}{m-1} p(q)^{m-1} (1-q)^{k-m}. \end{aligned}$$

Combining these probabilities, the expected ASR for UE is:

$$\begin{aligned} \mathbb{E}[\text{ASR}]_{\text{UE}} &= (1-p) \cdot (1-q)^{k-1} \cdot \frac{1}{k} \\ &+ \sum_{m=1}^k p \cdot \frac{1}{m} \cdot \binom{k-1}{m-1} q^{m-1} (1-q)^{(k-1)-(m-1)}. \end{aligned}$$

2) *SHE Protocol*: The expected ASR of SHE is defined as the probability that  $\hat{x} = x$ :

$$\mathbb{E}[\text{ASR}]_{\text{SHE}} = \Pr[\hat{x} = x] = \Pr \left[ y_x > \max_{i \neq x} y_i \right].$$

Define the random variables:

$$\begin{aligned} y_x &= 1 + Z_x, \quad \text{where } Z_x \sim \text{Laplace}(0, b), \\ y_i &= 0 + Z_i = Z_i, \quad \text{where } Z_i \sim \text{Laplace}(0, b), \quad \forall i \neq x \end{aligned}$$

All  $Z_i$  and  $Z_x$  are independent random variables. Let  $M = \max_{i \neq x} y_i = \max_{i \neq x} Z_i$ . Then, the expected ASR becomes:

$$\begin{aligned} \mathbb{E}[\text{ASR}]_{\text{SHE}} &= \Pr[y_x > M] \\ &= \Pr[1 + Z_x > M] \\ &= \Pr[Z_x > M - 1]. \end{aligned}$$

The cumulative distribution function (CDF) of the Laplace distribution  $Z_x \sim \text{Laplace}(0, b)$  is:

$$F_Z(z) = \begin{cases} \frac{1}{2} \exp\left[\frac{z}{b}\right], & \text{if } z \leq 0, \\ 1 - \frac{1}{2} \exp\left[-\frac{z}{b}\right], & \text{if } z > 0. \end{cases}$$

The probability density function (PDF) of  $Z_x$  is:

$$f_Z(z) = \frac{1}{2b} \exp\left[-\frac{|z|}{b}\right].$$

For  $M = \max_{i \neq x} Z_i$ , since  $Z_i$  are independent and identically distributed (i.i.d.), the CDF of  $M$  is:

$$F_M(m) = [F_Z(m)]^{k-1}. \quad (28)$$

The PDF of  $M$  is then:

$$f_M(m) = (k-1) [F_Z(m)]^{k-2} f_Z(m). \quad (29)$$

The ASR can be expressed as:

$$\mathbb{E}[\text{ASR}]_{\text{SHE}} = \int_{-\infty}^{\infty} \Pr[Z_x > m - 1] f_M(m) dm. \quad (30)$$

Since  $Z_x$  and  $M$  are independent,  $\Pr[Z_x > m - 1] = 1 - F_Z(m - 1)$ . Therefore:

$$\mathbb{E}[\text{ASR}]_{\text{SHE}} = \int_{-\infty}^{\infty} [1 - F_Z(m - 1)] f_M(m) dm. \quad (31)$$

**Empirical Estimation via Simulation.** In this work, we estimate the expected ASR in Equation (31) empirically using Monte Carlo simulations, following:

1) **Generate Samples:**

- Sample  $Z_x$  from Laplace(0,  $b$ ).
- Sample  $Z_i$  for  $i \neq x$  and compute  $M = \max_{i \neq x} Z_i$ .

2) **Compute Success Indicator:**

- For each sample, check if  $1 + Z_x > M$ .

3) **Estimate ASR:**

- The ASR is estimated as the proportion of times  $1 + Z_x > M$  holds over all samples.

3) *THE Protocol:* Following the attack strategy for THE in Section IV-E2, we have:

- **Event 0:** The bit corresponding to the user's value  $x$  is less than  $\theta$  (i.e., remains 0) and all other bits also remain 0.
  - The attacker's guess is uniformly distributed over all  $k$  possible values.
  - Success rate:  $\frac{1}{k}$ .
  - Probability:  $\Pr(\text{Event 0}) = (1-p)(1-q)^{k-1}$ .
- **Event 1:** The bit corresponding to the user's value  $x$  is greater than  $\theta$  (i.e., flips to 1) and  $m-1$  other bits also flip to 1.
  - The attacker's guess is uniformly distributed over the bits set to 1.
  - If  $m$  bits are set to 1, the success rate is  $\frac{1}{m}$ .
  - Probability:  $\Pr(\text{Event 1 with } m \text{ bits set to 1}) = \binom{k-1}{m-1} p(q)^{m-1} (1-q)^{k-m}$ .

Thus, by combining these two events, we can derive the expected ASR as:

$$\mathbb{E}[\text{ASR}]_{\text{THE}} = \Pr(\text{Event 0}) \cdot \frac{1}{k} + \sum_{m=1}^k \Pr(\text{Event 1 with } m \text{ bits set to 1}) \cdot \frac{1}{m}.$$

More formally, the probability calculations of each event are:

1) **Probability of Event 0:**

$$\Pr(\text{Event 0}) = (1-p)(1-q)^{k-1}.$$

2) **Probability of Event 1 with  $m$  bits set to 1:**

$$\Pr(\text{Event 1 with } m \text{ bits set to 1}) = \binom{k-1}{m-1} p(q)^{m-1} (1-q)^{k-m}.$$

Combining these probabilities, the expected ASR for THE is:

$$\mathbb{E}[\text{ASR}]_{\text{THE}} = (1-p)(1-q)^{k-1} \cdot \frac{1}{k} + \sum_{m=1}^k \binom{k-1}{m-1} p(q)^{m-1} (1-q)^{k-m} \cdot \frac{1}{m}.$$

Using  $X \sim \text{Binomial}(k-1, q)$  where  $M = X + 1$ , we apply:

$$\mathbb{E} \left[ \frac{1}{X+1} \right] = \frac{1 - (1-q)^k}{kq}.$$

Final closed-form expression:

$$\mathbb{E}[\text{ASR}]_{\text{THE}} = (1-p) \frac{(1-q)^{k-1}}{k} + \frac{p}{kq} (1 - (1-q)^k). \quad (32)$$

*B. Optimization Strategies for Parameter Selection*

This section provides a detailed overview of the multi-objective optimization strategies supported by our framework for selecting protocol parameters in adaptive LDP mechanisms. Given a Pareto frontier generated from exhaustive grid search [43], we apply six classical selection methods to identify the most suitable trade-off between Attacker Success Rate (ASR) and Mean Squared Error (MSE), as described in Section V-C. Each strategy interprets the frontier differently and is designed to meet distinct design goals [44].

- **Utopia Point Minimization:** Selects the Pareto point closest (in Euclidean distance) to the theoretical ideal point (0, 0), representing zero ASR and zero MSE. This method emphasizes proximity to perfect privacy and utility, making it a conceptually intuitive baseline.
- **Weighted Scalarization (Default):** Computes a scalarized objective as in Equation (23), using user-defined weights ( $w_{\text{ASR}}, w_{\text{MSE}}$ ). The point that minimizes this weighted sum is selected. This strategy is tunable, interpretable, and easy to implement, making it the default in our framework. As mentioned in the main paper, we set  $w_{\text{ASR}} = w_{\text{MSE}} = 0.5$  by default.
- **Elbow (Knee) Method:** Identifies the point on the frontier that exhibits the greatest curvature, corresponding to the location where further reductions in MSE yield diminishing returns in terms of ASR. It does so by maximizing the perpendicular distance from the frontier to the chord connecting the extreme points.
- **$\epsilon$ -Constraint Selection:** Filters the Pareto frontier to retain only points with ASR below a predefined threshold  $\epsilon_{\text{ASR}}$ , and among them selects the one with the lowest MSE. If no feasible point exists, the strategy defaults to the utopia point. This is particularly useful in privacy-critical settings where strict ASR bounds are imposed. We set  $\epsilon_{\text{ASR}} = 0.1$  by default.
- **Hypervolume Contribution:** Selects the Pareto point that contributes the most area (in 2D) to the dominated space relative to a reference point. This method emphasizes diversity and coverage of the solution set, making it attractive when the overall Pareto frontier spread is important. We set the reference point as (1.0, 1.0).
- **Augmented Tchebycheff Scalarization:** Minimizes the augmented Chebyshev objective:  $\max_i \{w_i f_i\} + \rho \sum_i w_i f_i$ , where  $f = (\text{ASR}, \text{MSE})$ ,  $w_i$  are normalized weights, and  $\rho$  is a small regularization factor. This approach balances worst-case performance and average cost, useful when robustness is a key concern. We set  $w_{\text{ASR}} = w_{\text{MSE}} = 0.5$  and  $\rho = 10^{-6}$  by default.

Figure 9 presents the parameters selected by each strategy across a range of  $\epsilon$  values and domain sizes  $k \in \{100, 1000, 10000\}$  (representing small, medium, and large

domains). These plots provide insights into the behavior and consistency of the selection methods. We observe that most strategies tend to select similar parameter values, particularly in the high-privacy and low-privacy regimes. In contrast, the Elbow method often diverges from the others due to its reliance on geometric curvature, which can result in unstable behavior across different settings. Overall, **Weighted Scalarization** offers a robust compromise, simple to implement, interpretable and tunable, making it the **default strategy** in our implementation. Nevertheless, our implementation supports all strategies, enabling practitioners to select methods that best align with their specific privacy, utility or robustness requirements.

#### C. Additional Analytical Results for the ASR vs. MSE Trade-Off

To complement the results of Figure 5 (medium to low privacy regimes and small domain size) in Section VI-D, Figures 10 to 14 illustrate the ASR-MSE trade-off considering:

- Figure 10: high privacy regime and small domain size.
- Figure 11: high privacy regime and medium domain size.
- Figure 12: high privacy regime and large domain size.
- Figure 13: medium to low privacy regimes and medium domain size.
- Figure 14: medium to low privacy regimes and large domain size.

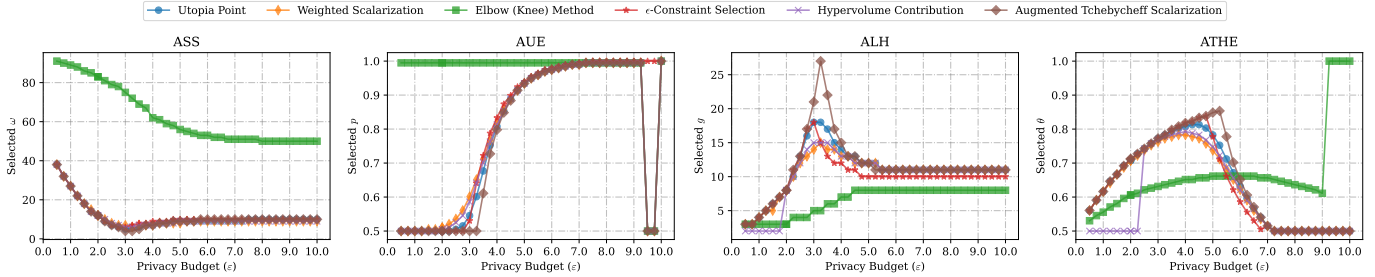
#### D. Additional Empirical Results for the ASR vs. MSE Trade-Off

To complement the results presented in Figure 8 (**Adult** dataset [46] with  $n = 48842$  and  $k = 100$  for the Age

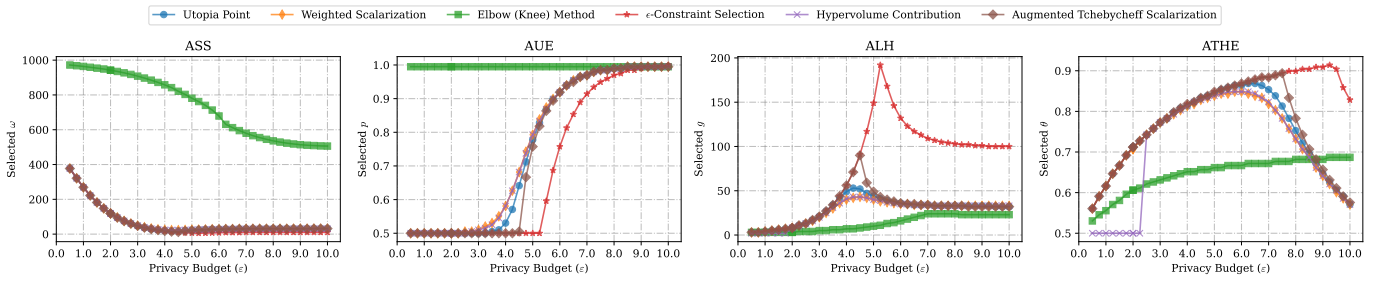
attribute), we now conduct experiments using a synthetic dataset generated from a Dirichlet distribution with parameter 1. Specifically, we compare empirical results obtained with varying numbers of users against analytical predictions computed using our closed-form equations from Section V-D. Similar to Figure 1, Figure 15 presents the empirical Pareto frontiers for the same protocols across different user counts ( $n \in \{5000, 50000, 500000\}$ ). Each subplot of Figure 15 evaluates the trade-off between ASR and MSE under varying privacy budgets  $\epsilon \in (2, 10)$  and a fixed domain size  $k = 100$ .

**Consistency across user counts:** Notably, Figure 15 shows that while the absolute variance (MSE) scales inversely with the number of users, the overall shape of the ASR-MSE Pareto frontier remains consistent across different values of  $n$ . This behavior aligns with theoretical expectations, as increasing the number of users reduces the variance but does not alter the fundamental trade-off between privacy and utility.

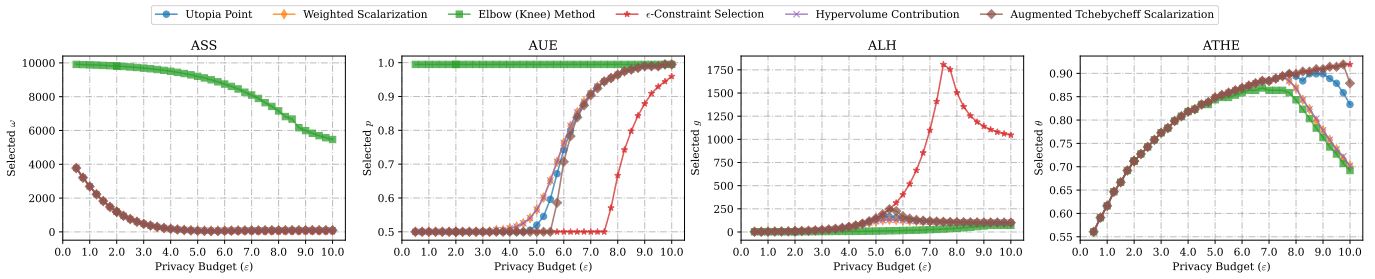
**Empirical and analytical alignment:** Similar to the results in Figure 8, the empirical ASR-MSE trends in Figure 15 closely follow the analytical ones in Figure 1, reinforcing the validity of our closed-form equations across various dataset distributions and user settings. These findings confirm that our analytical framework provides a reliable approximation for real-world deployments of LDP protocols, allowing practitioners to anticipate privacy-utility trade-offs without requiring extensive empirical evaluations.



(a) Domain size  $k = 100$ .



(b) Domain size  $k = 1000$ .



(c) Domain size  $k = 10000$ .

Fig. 9: Selected protocol parameters across privacy budgets  $\epsilon$  for each adaptive mechanism (ASS, AUE, ALH, ATHE), under six multi-objective selection strategies. Each subplot considers a range of privacy budgets  $\epsilon \in (0.5, 10)$  and varying domain sizes  $k \in \{100, 1000, 10000\}$ . Each curve shows how a strategy (*e.g.*, Utopia Point, Weighted Scalarization, Elbow Method) selects optimal parameters from the Pareto frontier of (ASR, MSE) trade-offs. While most strategies converge to similar configurations, the Elbow method exhibits distinctive behavior due to its curvature-based criterion.

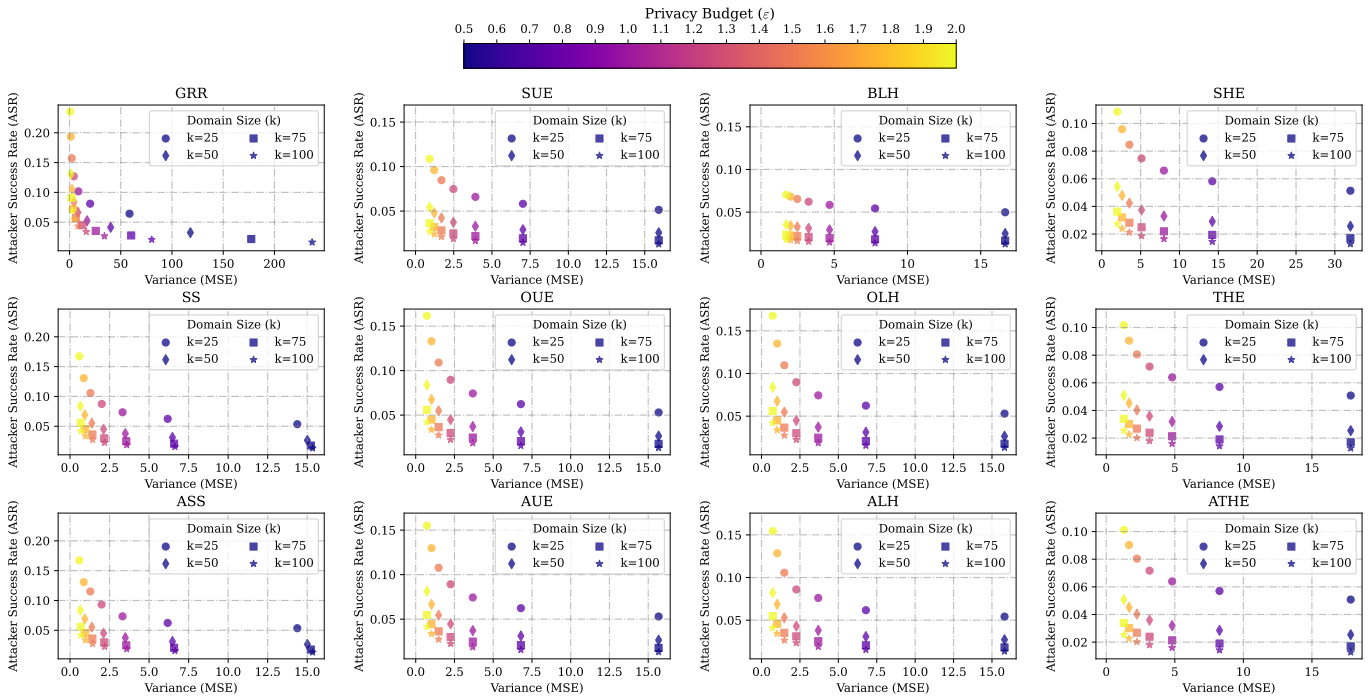


Fig. 10: Attacker Success Rate (ASR) vs. Variance (MSE) for numerous LDP frequency estimation protocols. Each plot shows how each protocol performs under varying privacy budgets  $\epsilon$  and domain sizes ( $k$ ), illustrating the trade-off between adversarial success rate (ASR) and utility (MSE). State-of-the-art LDP protocols (*i.e.*, GRR, SUE, BLH, SHE, SS, OUE, OLH, and THE) are compared against our adaptive counterparts (*i.e.*, ASS, AUE, ALH, and ATHE). Each point represents a different configuration of  $\epsilon$  (in high privacy regimes) and  $k$  (small domain), with colors indicating the privacy budget level.

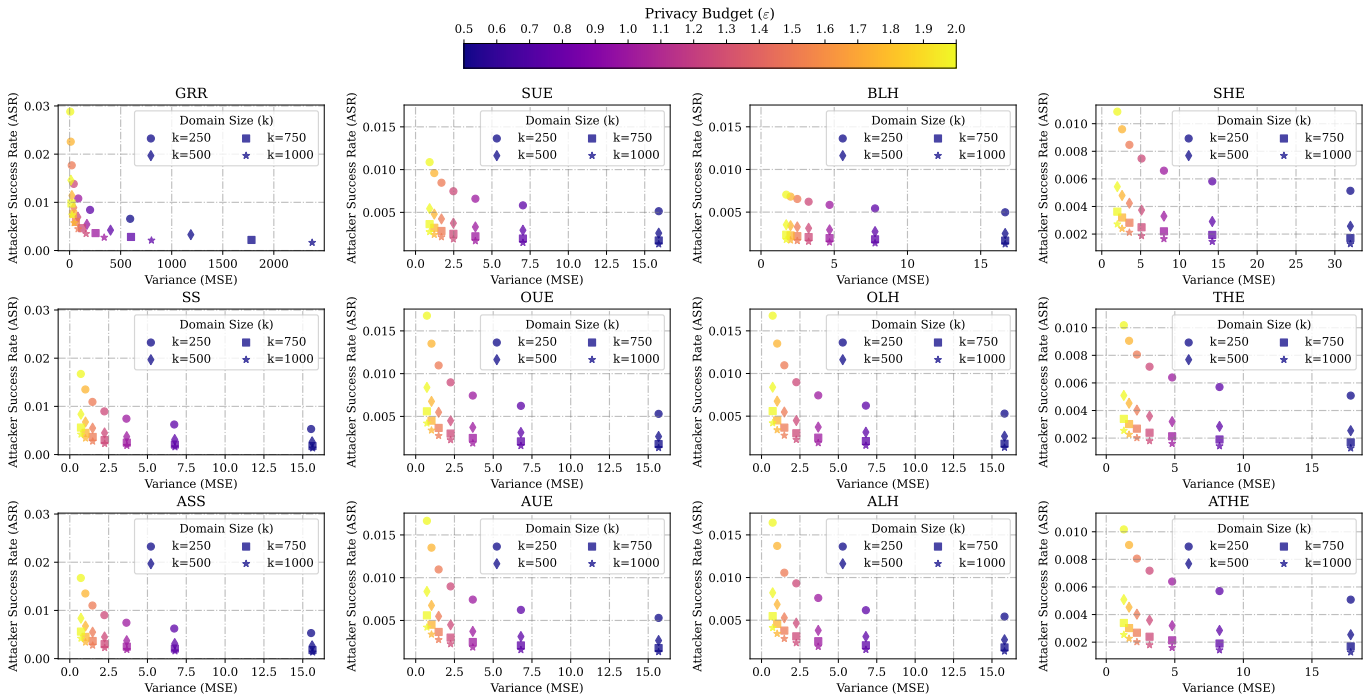


Fig. 11: Attacker Success Rate (ASR) vs. Variance (MSE) for numerous LDP frequency estimation protocols. Each plot shows how each protocol performs under varying privacy budgets  $\epsilon$  and domain sizes ( $k$ ), illustrating the trade-off between adversarial success rate (ASR) and utility (MSE). State-of-the-art LDP protocols (*i.e.*, GRR, SUE, BLH, SHE, SS, OUE, OLH, and THE) are compared against our adaptive counterparts (*i.e.*, ASS, AUE, ALH, and ATHE). Each point represents a different configuration of  $\epsilon$  (in high privacy regimes) and  $k$  (medium domain), with colors indicating the privacy budget level.

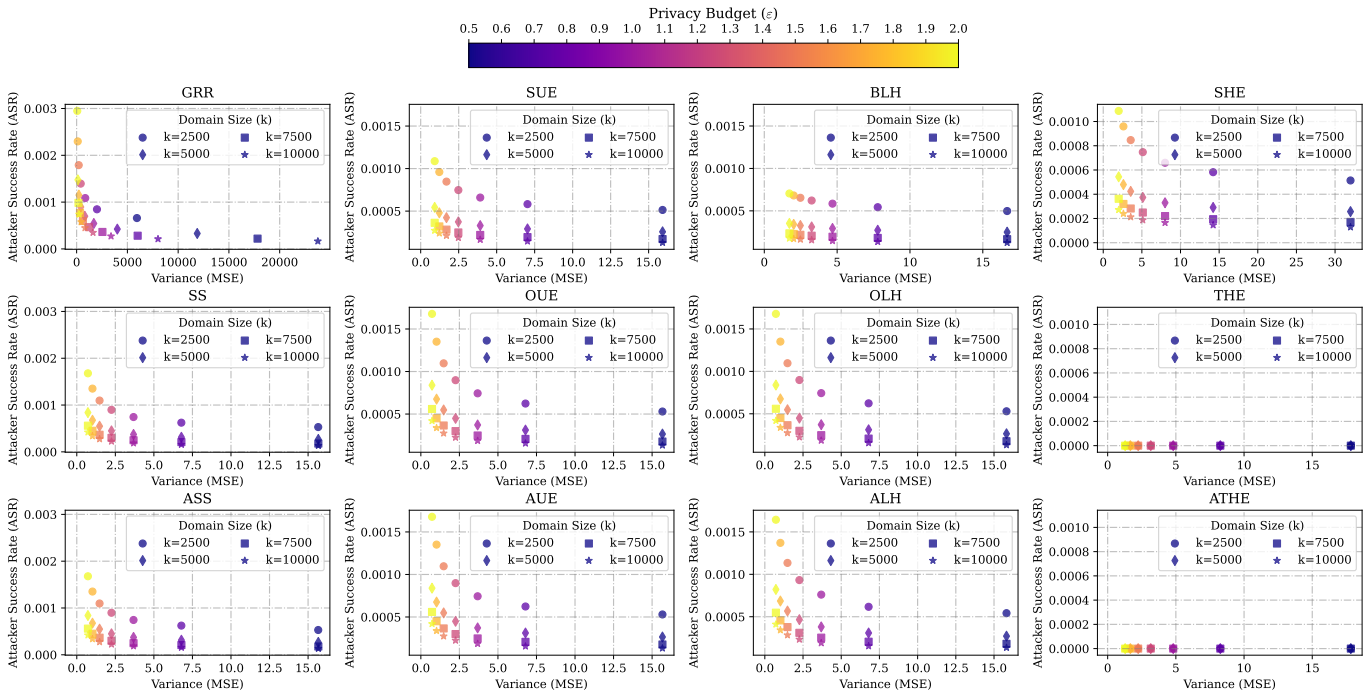


Fig. 12: Attacker Success Rate (ASR) vs. Variance (MSE) for numerous LDP frequency estimation protocols. Each plot shows how each protocol performs under varying privacy budgets  $\epsilon$  and domain sizes ( $k$ ), illustrating the trade-off between adversarial success rate (ASR) and utility (MSE). State-of-the-art LDP protocols (*i.e.*, GRR, SUE, BLH, SHE, SS, OUE, OLH, and THE) are compared against our adaptive counterparts (*i.e.*, ASS, AUE, ALH, and ATHE). Each point represents a different configuration of  $\epsilon$  (in high privacy regimes) and  $k$  (large domain), with colors indicating the privacy budget level.

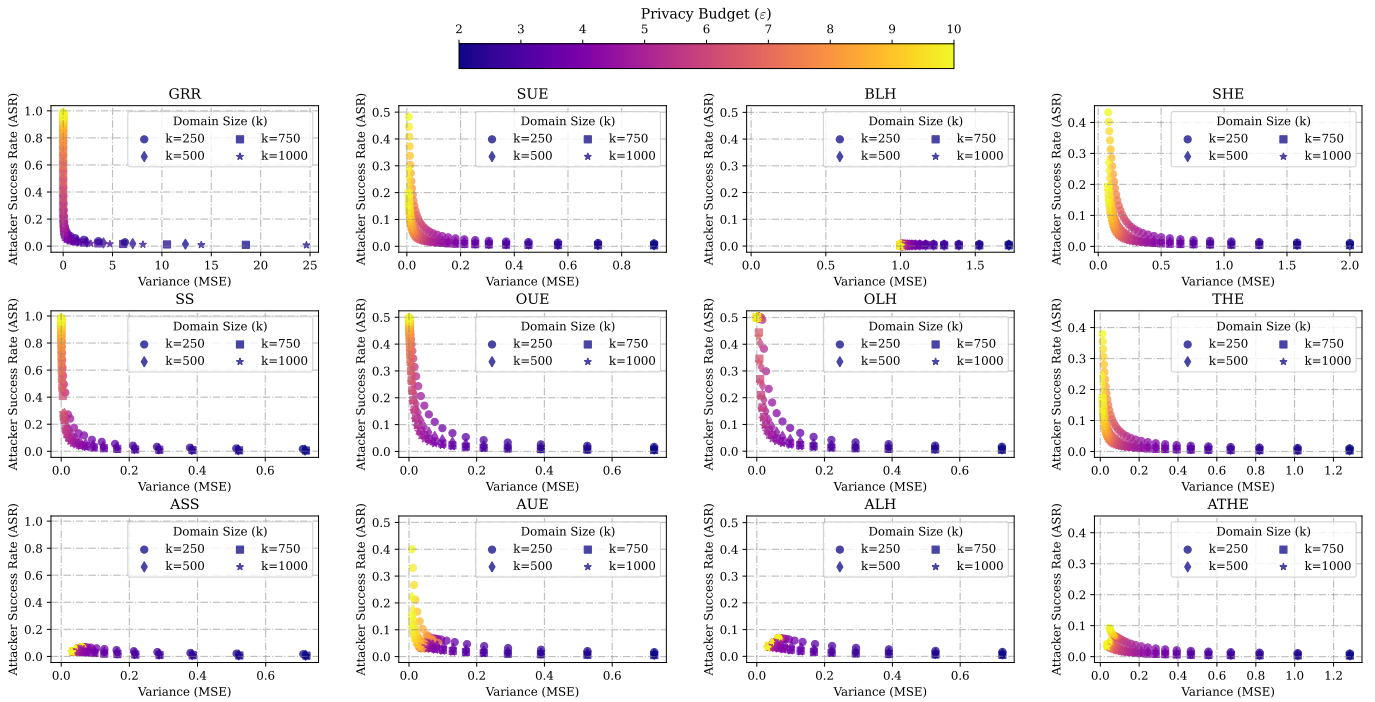


Fig. 13: Attacker Success Rate (ASR) vs. Variance (MSE) for numerous LDP frequency estimation protocols. Each plot shows how each protocol performs under varying privacy budgets  $\epsilon$  and domain sizes ( $k$ ), illustrating the trade-off between adversarial success rate (ASR) and utility (MSE). State-of-the-art LDP protocols (*i.e.*, GRR, SUE, BLH, SHE, SS, OUE, OLH, and THE) are compared against our adaptive counterparts (*i.e.*, ASS, AUE, ALH, and ATHE). Each point represents a different configuration of  $\epsilon$  (in medium to low privacy regimes) and  $k$  (medium domain), with colors indicating the privacy budget level.

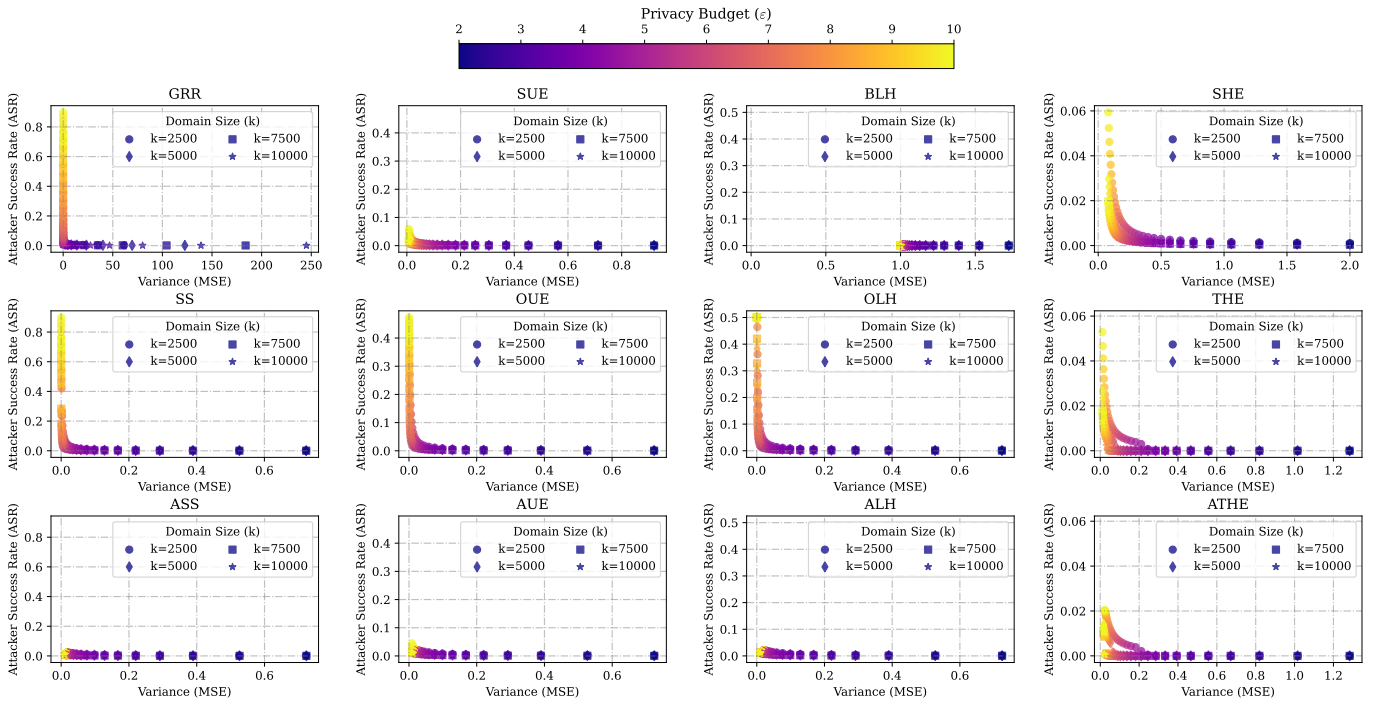
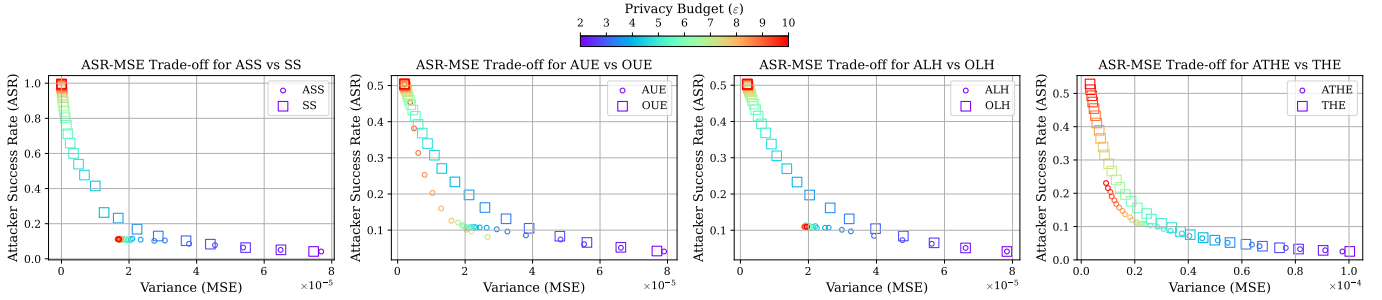
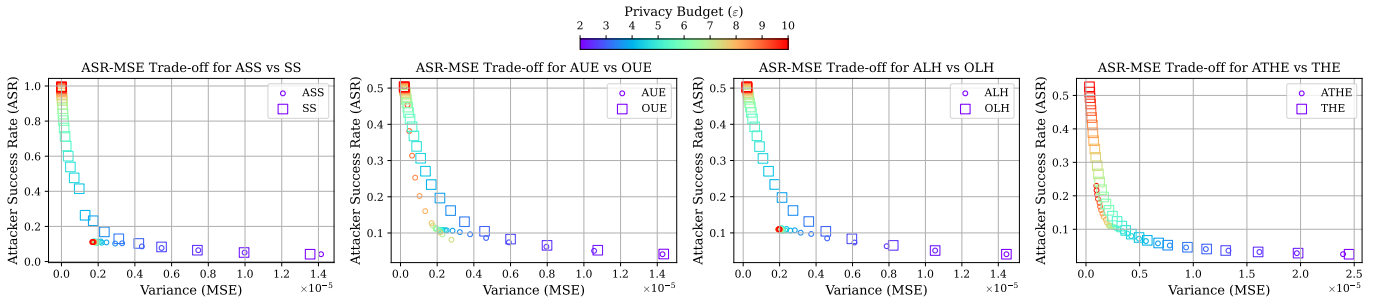


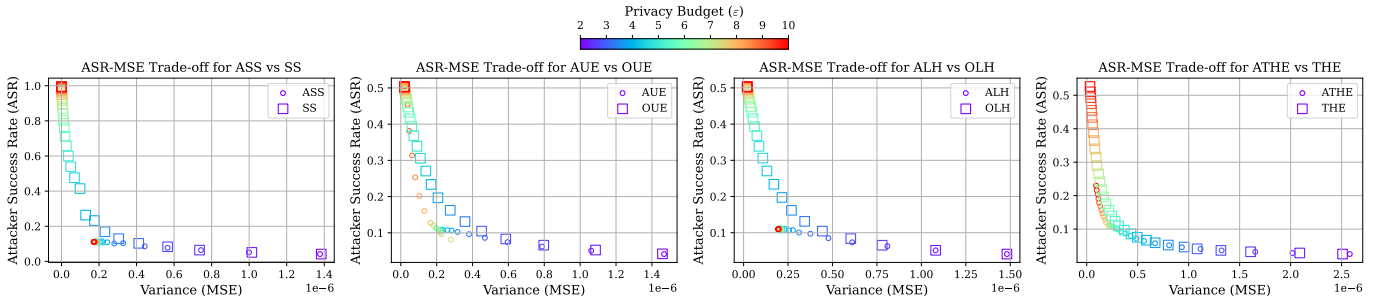
Fig. 14: Attacker Success Rate (ASR) vs. Variance (MSE) for numerous LDP frequency estimation protocols. Each plot shows how each protocol performs under varying privacy budgets  $\epsilon$  and domain sizes ( $k$ ), illustrating the trade-off between adversarial success rate (ASR) and utility (MSE). State-of-the-art LDP protocols (*i.e.*, GRR, SUE, BLH, SHE, SS, OUE, OLH, and THE) are compared against our adaptive counterparts (*i.e.*, ASS, AUE, ALH, and ATHE). Each point represents a different configuration of  $\epsilon$  (in medium to low privacy regimes) and  $k$  (large domain), with colors indicating the privacy budget level.



(a) Number of users  $n = 5000$ .



(b) Number of users  $n = 50000$ .



(c) Number of users  $n = 500000$ .

Fig. 15: Empirical comparison of ASR vs. MSE Pareto frontier for four state-of-the-art LDP protocols (*i.e.*, SS, OUE, OLH, and THE) and our proposed adaptive versions (*i.e.*, ASS, AUE, ALH, ATHE). Each subplot considers a range of privacy budgets  $\epsilon \in (2, 10)$ , a fixed domain size  $k = 100$ , and varying numbers of users  $n \in \{5000, 50000, 500000\}$ . The dataset follows a Dirichlet distribution with parameter 1. Results are averaged over 100 independent runs.